Supplementary Information

Versatile post-functionalisation strategy for the formation of modular organic-inorganic polyoxometalate hybrids

David E. Salazar Marcano,[1] Mhamad Aly Moussawi,[1] Alexander V. Anyushin,[1] Sarah Lentink,[1] Luc Van Meervelt,[1] Ivana Ivanović-Burmazović[2] and Tatjana N. Parac-Vogt[1]*

[1] Department of Chemistry, KU Leuven, Celestijnenlaan 200F, 3001 Leuven, Belgium
[2] Department of Chemistry, Ludwig-Maximilian-University, Butenandtstr. 5-13, Haus D, 81377 Munich, Germany

*E-mail: tatjana.vogt@kuleuven.be ; Tel: +32 (0)16 327612

Table of Contents

Characterisation Techniques

Nuclear Magnetic Resonance (NMR) Spectroscopy

All multinuclear 1D NMR spectra were acquired on Bruker Avance 400 and 600 spectrometers for samples in CD_3CN or D_2O at 25 °C. ^{1}H 2D DOSY NMR and the ^{1}H-^{13}C 2D HSQC spectra were acquired for 3 mM samples on a Bruker Avance 600 spectrometer using Bruker's ledpgs2 and hsqcedetgpsisp2.2 pulse programs respectively. Chemical shifts are reported relative to tetramethylsilane (TMS) for ^{1}H and ^{13}C NMR, 85% H_3PO_4 for ^{31}P NMR, $VOCl_3$ for ^{51}V NMR and 1 M $Al(NO_3)_3$ in D_2O for ^{27}Al NMR.

Fourier Transform – Infrared (FT-IR) Spectroscopy

FT-IR spectra of the solid samples were acquired with a Bruker Vertex 70 FT-IR spectrometer by attenuated total reflection.

Mass Spectrometry (MS)

Electrospray Ionisation MS (ESI-MS) spectra in the range 50-2000 *m/z* were obtained in negative ion mode on a Thermo Finnigan LCQ Advantage Mass Spectrometer with a quadrupole ion trap mass analyser and were then processed with the Xcalibur software. Cryospray-ionisation MS spectra were also acquired for the characterisation of the POM-POM hybrids using a UHR-TOF Bruker Daltonik maXis plus, an ESI-quadrupole time-of-flight (qToF) MS coupled to a Bruker Daltonik Cryospray unit. The temperatures of the spray gas and the dry gas (both N_2) were maintained at −40 °C and −35 °C, respectively. The samples were dissolved in acetonitrile (HPLC grade) and were injected directly via a syringe pump at a flow rate of 180 µL per hour. Detection was carried out in negative ion mode with a source voltage of 3.2 kV. The measured data were processed and analysed with the software Bruker Data Analysis 5.2.

Elemental Analysis

The Al, Cr, Mo, V, W elemental composition of samples was determined by atomic absorption with a Perkin Elmer ICP-OES Avio 500 after microwave assisted acid digestion. The samples were first mixed for 1 min with 5 mL HCl, 4 mL HNO_3, and 2 mL HBF_4 in a Teflon vessel. After 10 min, the vessel was sealed and the mixture was heated at 210 °C for 15 min in a MARS6 digestion microwave (15 min ramp time, 15 min hold and 30 min cooling). Before measuring, the mixtures were allowed to cool down and diluted with ultrapure water to obtain solutions with 2% HNO_3. The C, H, and N elemental composition of samples was determined with a Flash EA-2000 CHN elemental analyser. Samples were dried under vacuum at 50 °C overnight before elemental analysis.

UV-Vis Spectroscopy

UV-Vis spectra between 600 nm and 200 nm were acquired with an Agilent Cary 6000i UV-VIS-NIR spectrometer at room temperature using a scan rate of 600 nm/min. The spectra 10 µM solutions of the TBA-salts in acetonitrile and of the Na-salts in water were acquired to observe the LMCT bands. More concentrated solutions (400 µM or 200 µM) were also measured to be able to observe the weak absorbance peaks (e.g. d-d bands).

Thermogravimetric Analysis (TGA)

The thermal stability of the synthesised compounds was measured from 30 °C to 630 °C at a heating rate of 5 °C per minute under N_2 atmosphere with a NETZSCH STA 449 F3 Jupiter® thermal analyser.

Single Crystal X-ray Diffraction

X-ray intensity data were collected at 293(2) K using Mo Kα radiation (λ = 0.71073 Å) on an Agilent Supernova diffractometer, equipped with an Atlas CCD detector. The images were interpreted and integrated with CrysAlisPRO[1] and the implemented absorption correction was applied. The structures were solved using Olex2[2] with the ShelXT[3] structure solution program using Intrinsic Phasing and refined with the ShelXL[4] refinement package using full-matrix least-squares minimisation on F^2. Distance restraints (DFIX, DANG) were used for the tetrabutylammonium (TBA) moieties. All H atoms were placed in idealised positions and refined in the riding mode. Non-hydrogen atoms were anisotropically refined and the hydrogen atoms with isotropic temperature factors fixed at 1.2 times U_{eq} of the parent atoms (1.5 for methyl groups). Crystallographic data for **C** and **L** have been deposited with the Cambridge Crystallographic Data Centre and allocated the deposition numbers CCDC-2114104 and 2114105, respectively.

Table S1 Crystallographic parameters and refinement details for the crystal structures.

Compound	**C**	**L**
Formula	$C_{68}H_{146}O_{32}N_3Mo_6Cr$	$C_{26}H_{55}O_{13.5}NV_3$
FW, g.mol^{-1}	2145.52	750.53
T, K	293(2)	293(2)
crystal size (mm)	0.3 × 0.3 × 0.15	0.3 × 0.25 × 0.15
crystal system	Monoclinic	Monoclinic
space group	$P2_1/c$	$P2_1/c$
a, Å	27.8416 (11)	13.0520 (12)
b, Å	13.6571 (5)	13.4949 (9)
c, Å	25.0139 (8)	20.5929 (10)
β	92.128 (3)°	104.803 (8)°
V, Å^3	9504.6 (6)	3506.8 (4)
Z	4	4
ρ_{calc}, g.cm^{-3}	1.499	1.422
μ(Mo Kα), cm^{-1}	0.949	0.843
λ(Mo Kα), Å	0.71073	0.71073
2θ range	5.234° ≤ 2θ ≤ 50.504°	5.084° ≤ 2θ ≤ 49.426°
data collected	91482	38832
unique data	17207	5912
unique data I>2σ(I)	12455	3732
no. Parameters	1217	412
restraints	796	445
$R_w(F^2)$	0.1847	0.2460
R(F)	0.0850	0.0857
GOF	1.169	1.054

C crystallises in the centrosymmetric space group $P2_1/c$ where the asymmetric unit contains two halves of the POM and three TBA counter cations. The inorganic core of the structure exhibits a typical Anderson-Evans topology composed of six edge-sharing MoO_6 octahedra surrounding an edge-sharing CrO_6 octahedron in a planar arrangement (**Figure S1**). The oxygen atoms connecting these octahedra display three different coordination modes: (1) six triple-bridged oxygens (μ_3-O) each connecting the central heteroatom (Cr) to two out of the six hexagonally arranged (Mo) centres surrounding it, (2) six double-bridged oxygens (μ_2-O) connecting neighbouring (Mo)

addenda that, in collaboration with the (μ_3-O), form the edges shared between adjacent MoO_6 polyhedra, and finally (3) twelve terminal oxygen (O^t) atoms (two on each Mo centre). The discrete polyanion core is decorated by two dP ligands ((-$OHCH_2)_3CCH_2OCH_2C(CH_2OH)_3$) on opposite sides corresponding to the symmetrical bis-functionalised δ-isomer in which each triol group of the two organic ligands on either side of the POM is covalently attached to the POM core via three μ_3-O atoms. It should be noted that a splitting of two out of the three Mo atoms in one of the halves of the POM in the asymmetric unit has been observed (**Figure S1 (a)**) on two very close positions separated by 0.42 and 0.4 Å for Mo32•••Mo92 and Mo33•••Mo93 respectively, which represents a statistical occupancy factor of 0.84(4) (Mo32 and Mo33) and 0.16(4) (Mo92 and Mo93). This disorder imposed short bond lengths between the Mo atoms with 0.16(4) occupancy and the terminal oxygens (Mo93-O38 = 1.41 Å; Mo92-O35 = 1.55 Å). The following fragments also showed disorder and were refined as two parts with the sum of occupancies constrained to be unity: one of the dP substituents, the three terminal carbon atoms of each butyl chain of the TBA molecule containing N78, the two terminal carbon atoms of two butyl chains of the TBA molecule containing N95. For these disordered fragments also additional constraints on the atomic displacement factors (DELU, ISOR and EADP) were necessary.

The presence of three hydroxy groups on the free side of the ligand ensures a strong interaction between HPOM molecules in the same plane through an intermolecular network of hydrogen bonds between two of the hydroxy groups on one side of the triol and two terminal oxygens from an adjacent POM in the same column (average distance O^t•••OH = 2.794 Å), forming a chain. The third hydroxy group of the triol forms a hydrogen bond with a hydroxy group of a triol from an adjacent HPOM in a neighbouring column (average distance HO•••HO = 2.785 Å), thus forming a two-dimensional network of hydrogen bonds. Each hybrid POM contributes with all six of its hydroxy groups and four terminal oxygens to maintain the cohesion of this network. A network of short contacts also exists between the hydrogens of the TBA alkyl tails and the oxygens of the polyanion ($d_{C\text{-}H\ldots O\text{–}Mo}$ = 2.379–2.819 Å).

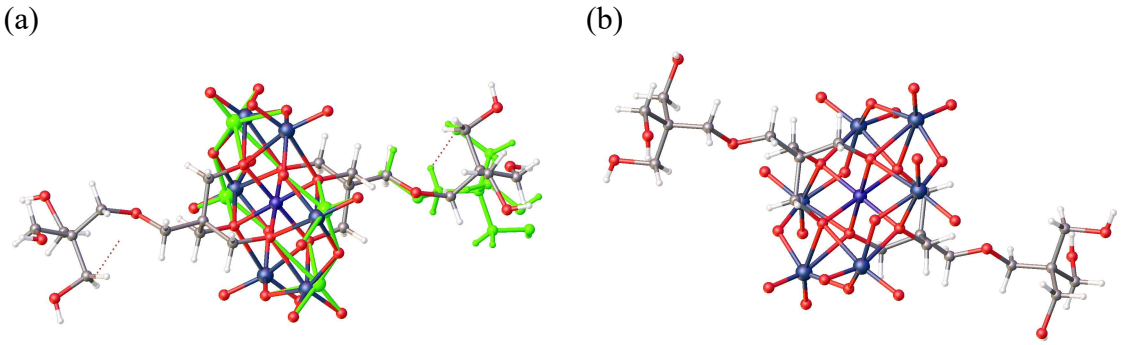

Figure S1 Ball-stick representation of $[CrMo_6O_{18}\{(OCH_2)_3CCH_2OCH_2C(CH_2OH)_3\}_2]^{3-}$ (**C**) without the TBA counter ions for clarity. The positional disorder of **C** observed in one half of the asymmetric unit is highlighted in green in (a) while the full structure of **C** without disorder is shown in (b). Hydrogen in white, carbon in grey, oxygen in red, nitrogen in navy blue, molybdenum in dark blue and chromium in purple.

L also crystalises in the centrosymmetric space group $P2_1/c$ space group. The asymmetric unit contains half the hybrid POM and one TBA cation (**Figure S2 (a)**). It displays a typical Lindqvist-type arrangement where six edge-sharing distorted VO_6 octahedra form an octahedral structure. The two dP ligands are attached in a trans configuration to opposite faces of the POM octahedron via three of the double-bridged oxygens (μ_2-O) on either side. The central oxygen bridging between the six metal centres (μ_6-O) corresponds to the inversion centre connecting all six vanadium atoms. Three atoms in the butyl chains of the TBA showed disorder and were refined with occupancies of 0.74(5):0.26(5) for C40 and 0.817(15):0.183(15) for C43 and C44 with equal atomic displacement factors for both positions (EADP). Enhanced rigid bond restraints (RIGU) were used for all atoms. The structure was refined as a two-component twin with fractions 0.766(4) and 0.234(4). Similar to **C**, the three-dimensional cohesion is maintained by a network of hydrogen bonds between OH groups of the ligand and terminal oxygens of an adjacent POM core along the *a* axis as well as a network of close contacts between the hydrogens of the alkyl tails of the four TBA cations surrounding the POM core and its surface oxygens ($d_{C\text{-}H\ldots O\text{–}V}$ = 2.367–2.841 Å) where each TBA cation lies between two POMs in the *bc* plane preserving the electroneutrality (**Figure S2 (b)**).

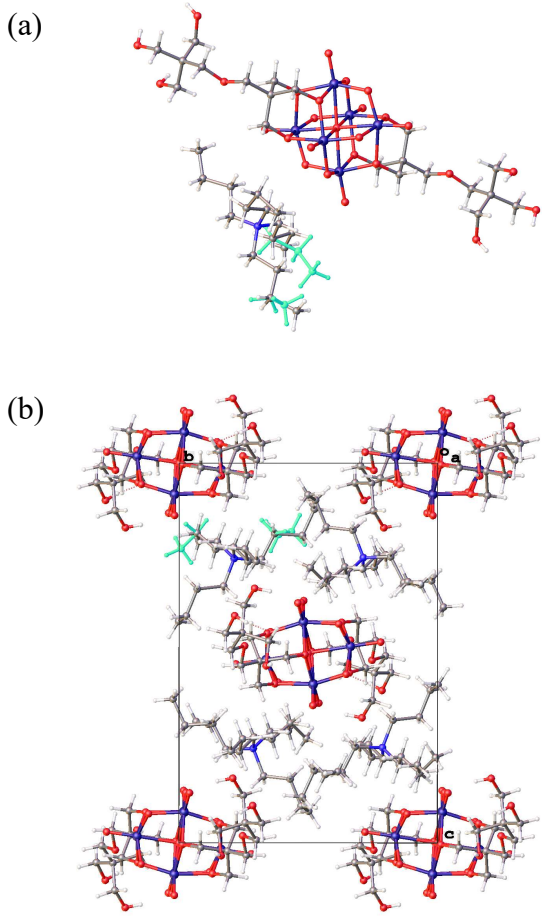

Figure S2 Ball-stick representation of $[V_6O_{13}\{(OCH_2)_3CCH_2OCH_2C(CH_2OH)_3\}_2]^{2-}$ (**L**) and the TBA counter ions in (a) the asymmetric unit including the positional disorder of the TBA counter cation and (b) the full unit cell viewed along the *bc* plane. Hydrogen in white, carbon in grey, oxygen in red, nitrogen in navy blue and vanadium in dark blue.

Synthesis & Characterisation

All reagents and solvents were used as obtained from commercial sources without further purification. The HPOM precursors $Na_3[Cr(OH)_6Mo_6O_{18}]\cdot 8H_2O$ ($CrMo_6$), $TBA_5H_4[P_2V_3W_{15}O_{62}]$ (**D**), $Na_3(H_2O)_6[Al(OH)_6Mo_6O_{18}]\cdot 2H_2O$ (**A**) used in the synthesis of **C**, **DLD**, **DCD**, **ALA**, and **ACA** were synthesised and characterised following published procedures.[5-7]

Synthesis of $TBA_2[V_6O_{13}\{(OCH_2)_3CCH_2OCH_2C(CH_2OH)_3\}_2]$ – TBA-L

TBA-L was synthesised based on a procedure adapted from the literature.[8] Sodium metavanadate (33 mmol) was dissolved in 150 mL of hot demineralised water giving a pale yellow solution with pH around 8.9. Then, the solution was cooled down to room temperature and the pH was adjusted to 3.0 by dropwise addition of around 30 mL of 1 M HCl resulting in the formation of an orange solution. Dipentaerythritol (11 mmol) was then added to the reaction mixture and it was placed under reflux for 5 days. After 5 days, the reaction was stopped, allowed to cool down to room temperature and filtered to remove small amounts of a brown precipitate. Tetrabutylammonium bromide (22 mmol) was dissolved in 20 mL of demineralised water and was then added dropwise to the clear red-orange filtrate under vigorous stirring, which resulted in the formation of a dark orange precipitate. The precipitate was filtered off on a glass frit under suction and washed with ice-cold water (2× 10 mL), ice-cold ethanol (2× 5 mL), diethyl ether (2× 20 mL), and then centrifuged. The obtained product was air dried for 3 days. Dark orange single crystals were obtained by vapor diffusion of diethyl ether into a solution of the product in methanol/acetonitrile. Yield: 3.13g, 37.9%.

Elemental analysis (%) for $C_{52}H_{110}N_2O_{27}V_6$ (1501.08 $gmol^{-1}$): calcd. = C 41.61, H 7.39, N 1.87; found = C 41.77, H 7.36, N 1.84.

ESI-MS (negative mode, CH_3CN, L = $[V_6O_{13}\{(OCH_2)_3CCH_2OCH_2C(CH_2OH)_3\}_2]^{2-}$): m/z = 508.1 ($[L]^{2-}$, calcd. m/z = 507.9), 1016.8 ($[L+H]^-$, calcd. m/z = 1016.8), 1258.0 ($[L+TBA]^-$, calcd. m/z = 1258.1).

FT-IR: $\tilde{\nu}$ (cm^{-1}) = 3378 (ν O-H, m), 2961 (ν C-H, m), 2938 (ν C-H, m), 2873 (ν C-H, m), 1644 (w), 1481 (δ C-H, m), 1463 (δ C-H, m), 1379 (δ C-H, m), 1304 (w), 1247 (w), 1192 (w), 1137 (ν C-O, m), 1037 (ν C-O, s), 953 (ν V=O, vs), 885 (w), 810 (ν V-O-V, s), 791 (ν V-O-V, s), 709 (ν V-O-V, vs), 580 (s), 513(s), 480 (s), 464 (s), 417 (vs).

^{1}H NMR (600 MHz, CD_3CN): δ (ppm) = 0.97 (t, 24 H, TBA CH_3), 1.37 (m, 16 H, TBA CH_2), 1.63 (m, 16 H, TBA CH_2), 3.13 (m, 16 H, TBA N-CH_2), 3.29 (s, 4 H, CH_2-O-CH_2), 3.31 (s, 4 H, CH_2-O-CH_2), 3.46 (s, 12 H, CH_2-OH), 5.04 (s, 12 H, CH_2-O-V).

^{13}C NMR (151 MHz, CD_3CN): δ (ppm) = 13.80 (TBA CH_3), 20.31 (TBA CH_2), 24.34 (TBA CH_2), 40.92 ($C(CH_2O\text{-})_3$), 46.37 ($C(CH_2O\text{-})_3$), 59.29 (TBA N-CH_2), 63.70 (CH_2-OH), 72.25 (CH_2-O-CH_2), 73.14 (CH_2-O-CH_2), 84.72 (CH_2-O-V).

^{51}V NMR (158 MHz, CD_3CN): δ (ppm) = -496.94 (s).

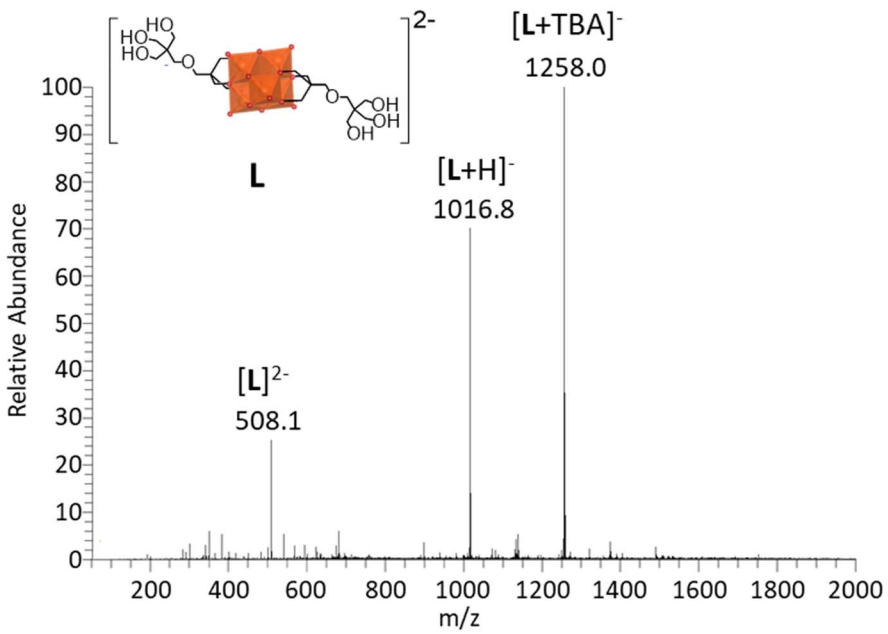

Figure S3 Negative mode ESI-MS spectrum of **L**.

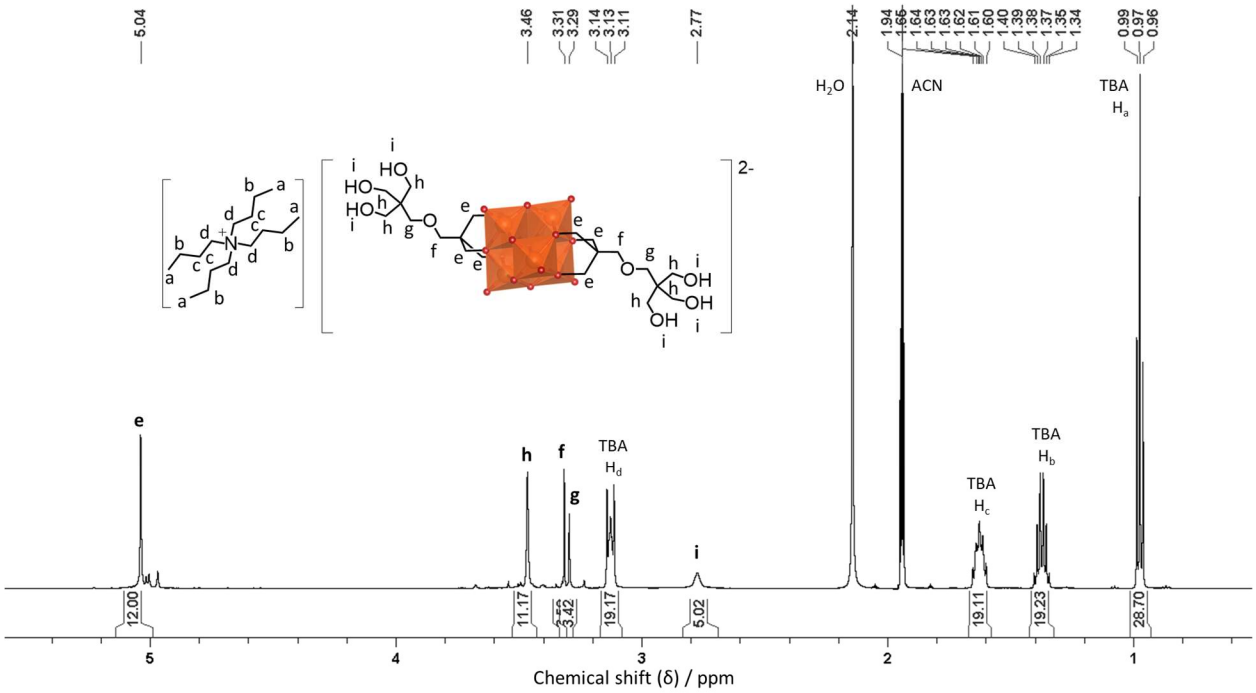

Figure S4 ^{1}H NMR spectrum of **L** in CD_3CN.

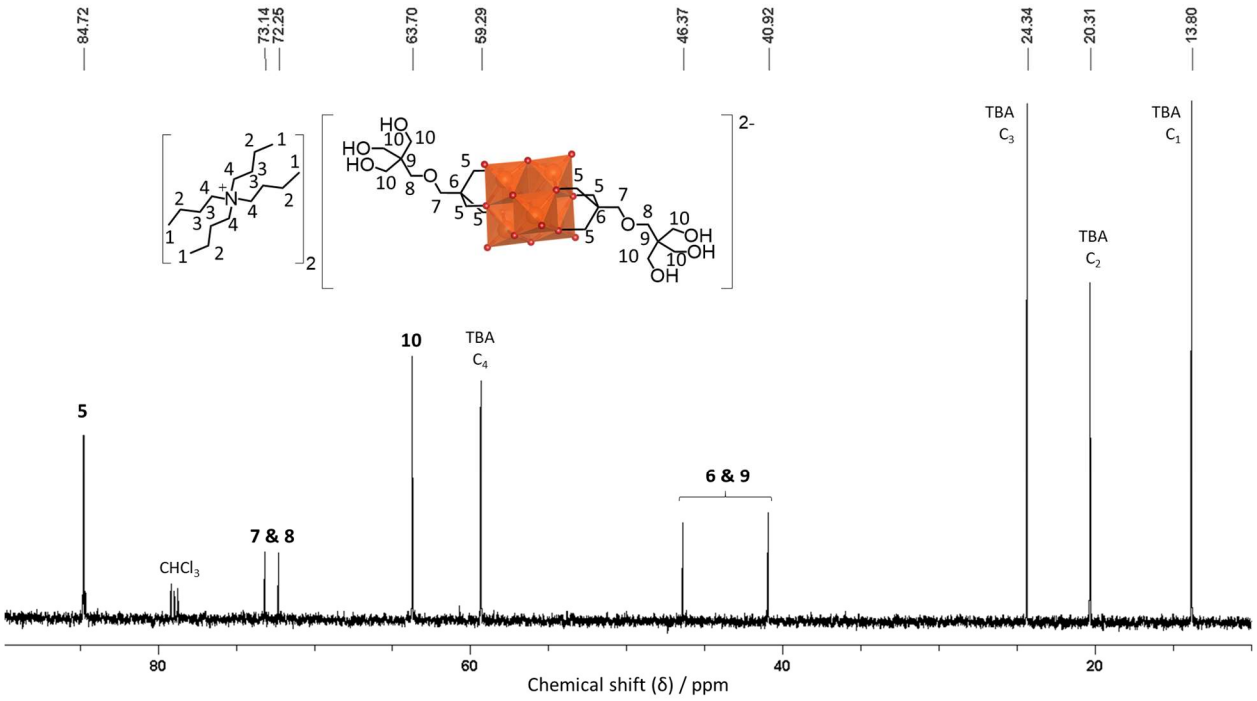

Figure S5 ^{13}C NMR spectrum of **L** in CD_3CN.

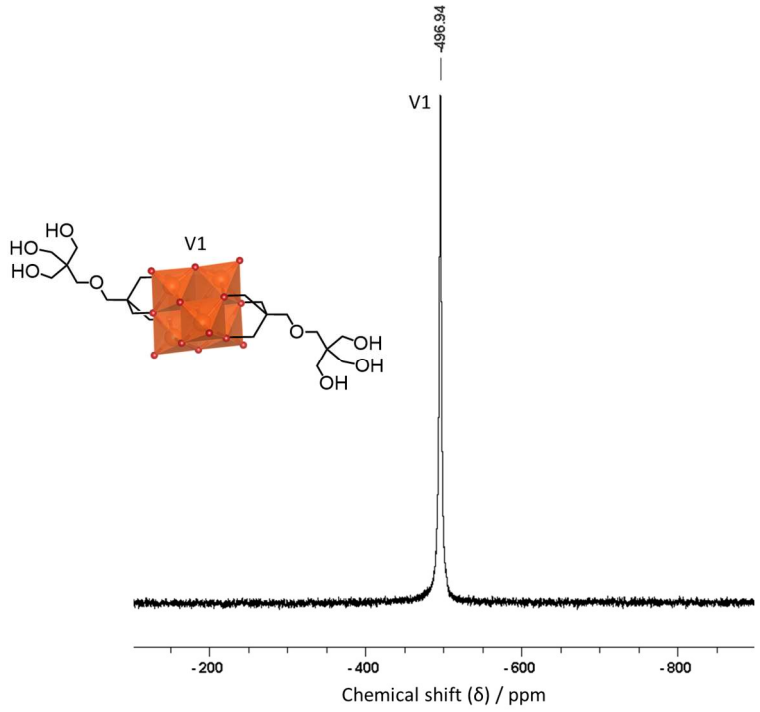

Figure S6 ^{51}V NMR spectrum of **L** in CD_3CN.

Synthesis of $TBA_3[CrMo_6O_{18}\{(OCH_2)_3CCH_2OCH_2C(CH_2OH)_3\}_2]$ – TBA-C

$Na_3[Cr(OH)_6Mo_6O_{18}]\cdot 8H_2O$ (2.0 mmol) and dipentaerythritol (8.0 mmol) were dissolved in 30 mL of hot demineralised water giving a transparent pink solution. This solution was sealed in a stainless steel reactor with Teflon lining and allowed to react at 160 °C for 7 days. Then, the reaction mixture was cooled down to room temperature, diluted by adding 20 mL of demineralised water, and filtered to remove a small amount of dark brown precipitate. Solid tetrabutylammonium bromide (15.0 mmol) was added to the filtrate (a clear pink solution) while vigorously stirring it. The pink precipitate was filtered off and washed with 10 mL of ice-cold demineralised water. It was then purified by dissolving it twice in 20 mL of hot methanol and re-precipitating it with 200 mL of diethyl ether. Then, it was washed with diethyl ether (2× 30mL) and dried under dynamic vacuum at 50 °C overnight. Pink crystals were obtained by vapor diffusion of diethyl ether into a solution of the product in ethanol. Yield: 2.65 g, 61.4%.

Elemental analysis (%) for $C_{68}H_{146}N_3O_{32}CrMo_6$ (2145.52 $gmol^{-1}$): calcd. = C 38.07, H 6.86, N 1.96, Mo 26.83, Cr 2.42; found = C 38.29, H 6.83, N 1.90, Mo 28.25, Cr 2.46.

ESI-MS (negative mode, CH_3CN, C = $[CrMo_6O_{18}\{(OCH_2)_3CCH_2OCH_2C(CH_2OH)_3\}_2]^{3-}$): 830.4 ($[C+TBA]^{2-}$, calcd. m/z = 830.3), 1662.6 ($[C+TBA+H]^-$, calcd. m/z = 1661.6), 1901.8 ($[C+2TBA]^-$, calcd. m/z = 1903.1).

FT-IR: $\tilde{\nu}$ (cm^{-1}) = 3419 (ν O-H, w), 2958 (ν C-H, m), 2931 (ν C-H, m), 2874 (ν C-H, m), 1481 (δ C-H, m), 1380 (δ C-H, w), 1159 (w), 1130 (ν C-O, m), 1016 (ν C-O, s), 937 (ν Mo=O, s), 912 (ν Mo=O, s), 897 (ν Mo=O, s), 814 (w), 739 (w), 650 (ν Mo-O-Mo, vs), 567 (s), 515 (m), 459 (m), 419 (m).

^{13}C NMR (151 MHz, CD_3CN): δ (ppm) = 13.93 (TBA CH_3), 20.45 (TBA CH_2), 24.36 (TBA CH_2), 46.08 ($C(CH_2O\text{-})_3$), 59.27 (TBA N-CH_2), 64.21 (CH_2-OH), 74.41 (CH_2-O-CH_2).

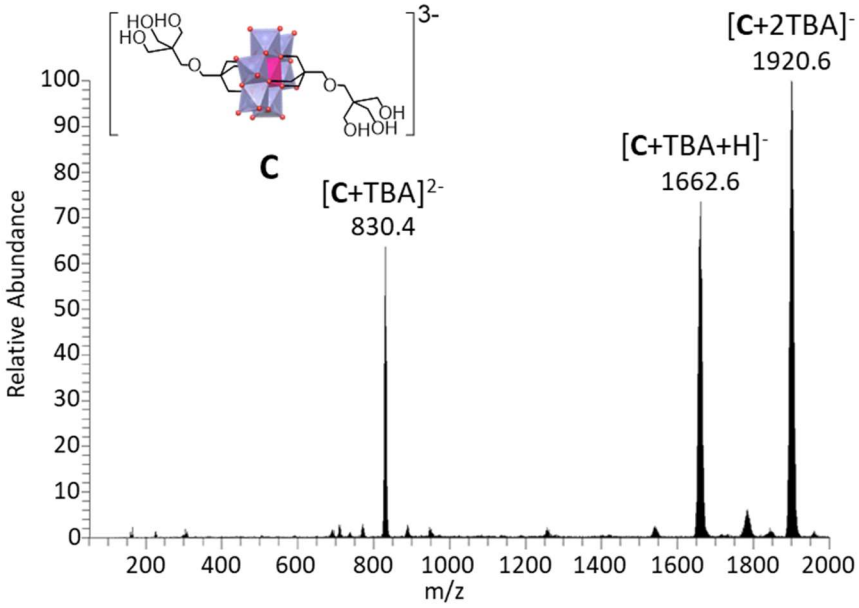

Figure S7 Negative mode ESI-MS spectrum of **C**.

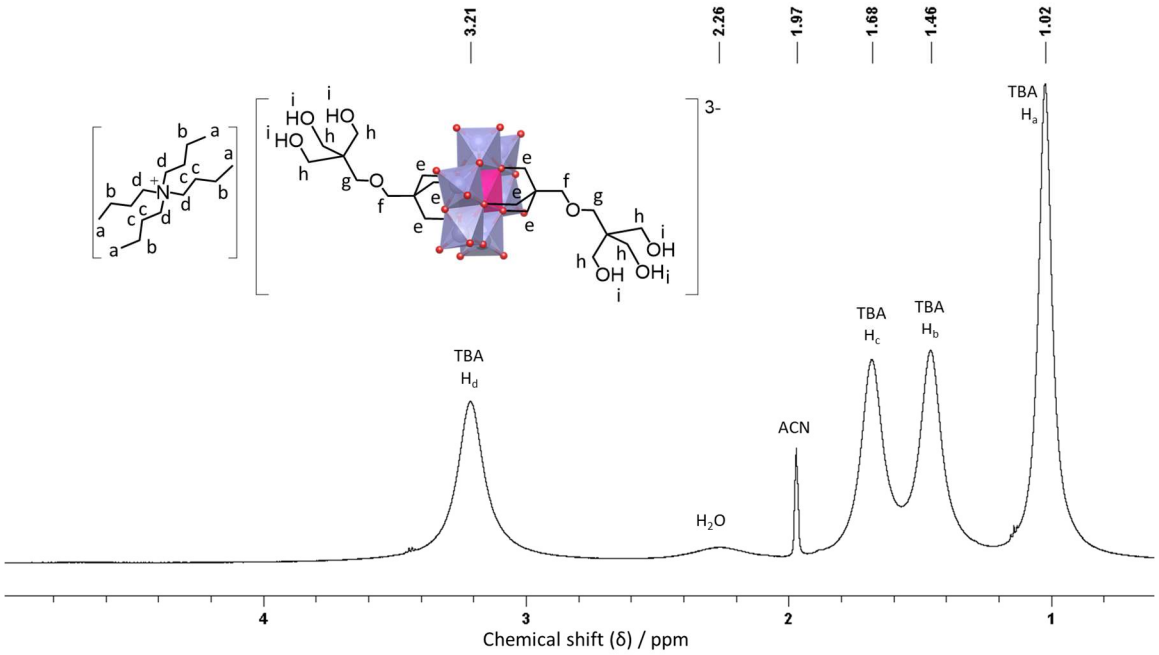

Figure S8 ^{1}H NMR spectrum of **C** in CD_3CN.

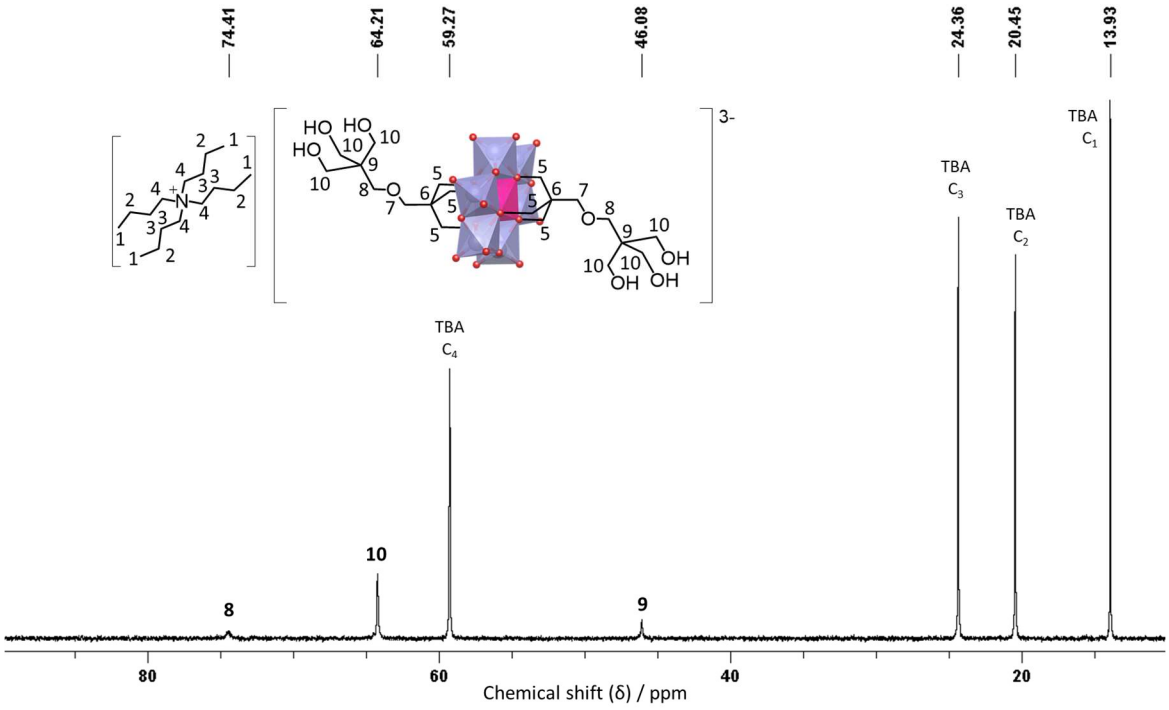

Figure S9 ^{13}C NMR spectrum of **C** in CD_3CN.

Ion metathesis of L & C

The Na-salts of **L** and **C** used for the synthesis of **ALA** and **ACA** were obtained by an ion metathesis procedure based on previously reported procedures.[9] **TBA-C** (0.25 mmol) was dissolved in a minimum amount of acetonitrile (8 mL) and it was mixed with sodium perchlorate (5 mmol) resulting in precipitation of the Na-salt. Due to the low solubility of **TBA-L** in acetonitrile, it was not dissolved in a minimum amount of acetonitrile and instead **TBA-L** (0.37 mmol) was mixed with sodium perchlorate (7.45 mmol) in 10 mL of acetonitrile for 2 h. In both cases, the precipitate formed was separated by centrifugation and washed several times with a small amount of acetonitrile. The pure product was then dried under dynamic vacuum at 50 °C overnight. The successful formation of the Na-salts was confirmed by FT-IR and by NMR for **L** (**Figure S11-S8**).

Na-L

FT-IR: $\tilde{\nu}$ (cm^{-1}) = 3381 (ν O-H, m), 2860 (ν C-H, w), 1627 (w), 1463 (δ C-H, w), 1444 (w), 1390 (w), 1370 (δ C-H, w), 1302 (w), 1190 (w), 1132 (ν C-O, m), 1020 (ν C-O, s), 946 (ν V=O, vs), 808 (ν V-O-V, s), 786 (ν V-O-V, s), 690 (ν V-O-V, vs), 564 (s), 495 (s), 461 (s), 407 (vs).

^{1}H NMR (400 MHz, D_2O): δ = 3.42 (s, 4 H, CH_2-O-CH_2), 3.52 (s, 4 H, CH_2-O-CH_2), 3.57 (s, 12 H, CH_2-OH), 5.26 (s, 12 H, CH_2-O-V).

^{51}V NMR (105 MHz, D_2O): δ = -506.92 ppm

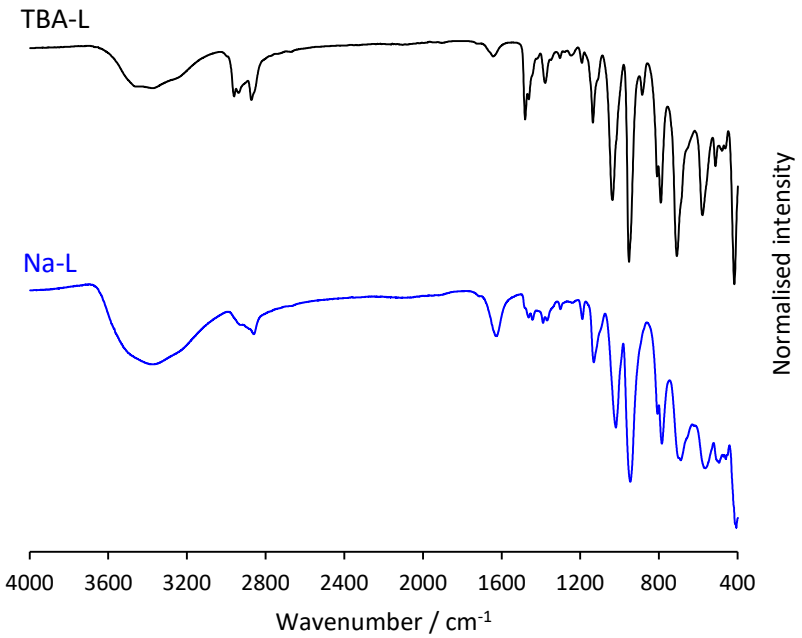

Figure S10 FT-IR spectra of **TBA-L** (top; black) and **Na-L** (bottom; blue).

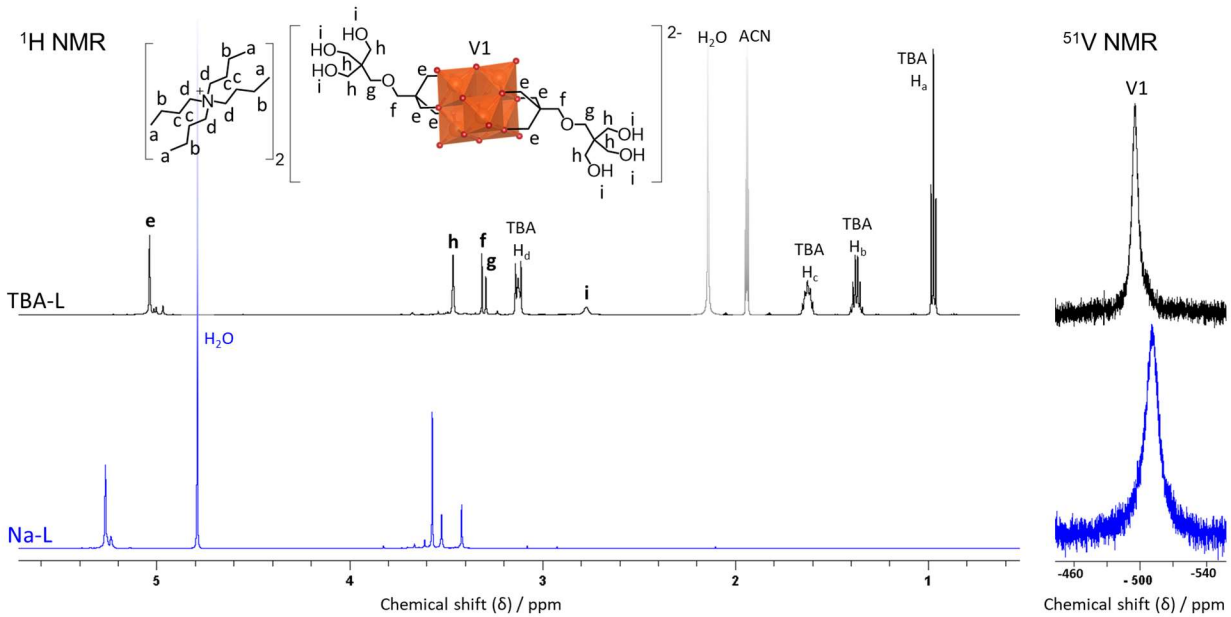

Figure S11 ^{1}H and ^{51}V NMR spectra of **TBA-L** in CD_3CN (top; black) and **Na-L** in D_2O (bottom; blue).

Na-C

FT-IR: $\tilde{\nu}$ (cm^{-1}) = 3408 (ν O-H, m), 2938 (ν C-H, w), 2919 (ν C-H, w), 2877 (ν C-H, w), 1633 (w), 1468 (δ C-H, m), 1452 (w), 1394 (δ C-H, w), 1367 (w), 1312 (w), 1286 (w), 1237 (w), 1190 (m), 1126 (ν C-O, m), 1003 (ν C-O, s), 933 (ν Mo=O, s), 901 (ν Mo=O, s), 816 (w), 635 (ν Mo-O-Mo, vs), 565 (s), 517 (vs), 461 (vs), 423 (vs).

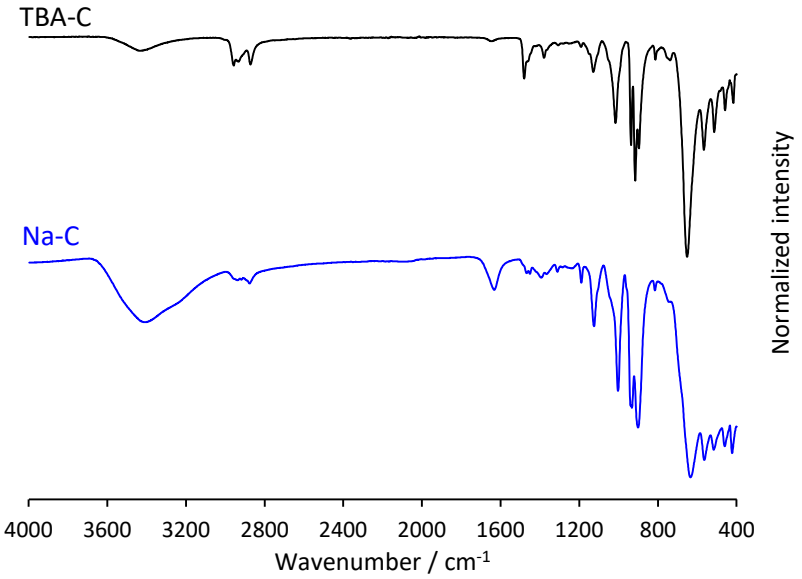

Figure S12 FT-IR spectra of **TBA-C** (top; black) and **Na-C** (bottom; blue).

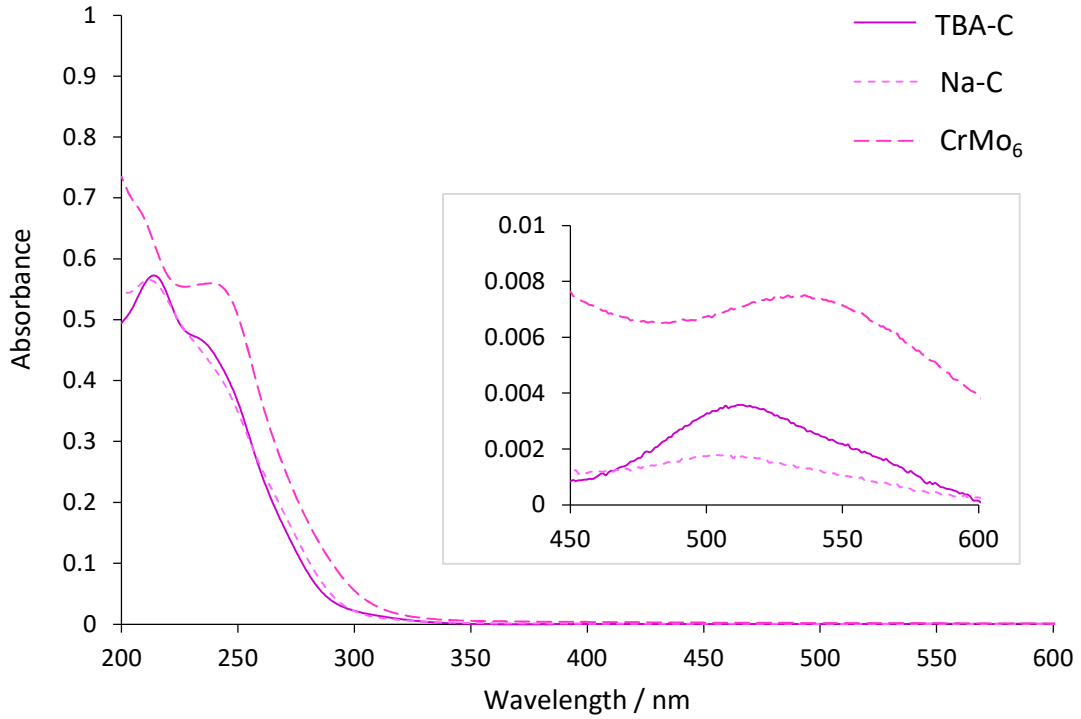

Figure S13 UV-Vis spectra of **TBA-C**, **Na-C** and **CrMo$_6$**.

Synthesis of $TBA_{11.4}H_{2.6}[V_6O_{13}\{(OCH_2)_3CCH_2OCH_2C(CH_2O)_3(P_2V_3W_{15}O_{59})\}_2]$ – DLD
$TBA_5H_4[P_2V_3W_{15}O_{62}]$ (0.2 mmol) and **TBA-L** (0.1 mmol) were dissolved in dry acetonitrile (30 mL) and placed under reflux in an Ar atmosphere for 7 days in the absence of light, by covering the round bottom flask with aluminium foil. The obtained orange solution was allowed to cool down to room temperature, filtered, and added dropwise to 160 mL of diethyl ether leading to the formation of an orange precipitate. The crude product was washed with ethanol (2× 10 mL) and diethyl ether (2× 20mL). It was then dissolved in a minimum volume of acetonitrile and this solution was added dropwise to 80 mL of diethyl ether leading to the formation of a dark yellow precipitate. The precipitate was collected by centrifugation and dried under dynamic vacuum at 50 °C overnight. Yield: 1.05 g, 95.3%.

Elemental Analysis (%) for $C_{202.4}H_{445}N_{11.4}O_{145}P_4V_{12}W_{30}$ (11609.48 $gmol^{-1}$): calcd. = C 20.94, H 3.86, N 1.38, V 5.27 and W 47.51; found = C 21.09, H 3.86, N 1.38, V 5.30 and W 49.33.

FT-IR: $\tilde{\nu}$ (cm^{-1}) = 3486 (ν O-H, w), 2960 (ν C-H, m), 2933 (ν C-H, m), 2872 (ν C-H, m), 1632 (w), 1481 (δ C-H, m), 1465 (δ C-H, m), 1380 (δ C-H, w), 1190 (w), 1130 (ν C-O, w), 1084 (ν P-O, s), 1062 (ν C-O, m), 1002 (w), 988 (w), 947 (ν M=O, vs), 906 (ν W-O-W, vs), 797 (ν M-O-M, vs), 718 (ν V-O-V, vs), 597 (s), 525 (s), 477 (s), 421 (s). M = V or W.

^{1}H NMR (600 MHz, CD_3CN): δ (ppm) = 1.00 (t, 144 H, TBA CH_3), 1.42 (m, 96 H, TBA CH_2), 1.66 (m, 96 H, TBA CH_2), 3.18 (m, 96 H, TBA N-CH_2), 3.36 (s, 4 H, CH_2-O-CH_2), 3.44 (s, 4 H, CH_2-O-CH_2), 5.08 (s, 12 H, CH_2-O-V_6), 5.45 (s, 12 H, CH_2-O-V_3).

^{13}C NMR (151 MHz, CD_3CN): δ (ppm) = 13.94 (TBA CH_3), 20.38 (TBA CH_2), 24.40 (TBA CH_2), 42.50 (C(CH_2O-)$_3$), 59.28 (TBA N-CH_2), 72.30 (CH_2-O-CH_2), 85.05 (CH_2-O-V_6), 88.66 (CH_2-O-V_3).

^{31}P NMR (243 MHz, CD_3CN): δ (ppm) = -7.51 (s, 2P, $\Delta\nu_{1/2}$ = 4.1 Hz); -13.55 (s, 2P, $\Delta\nu_{1/2}$ = 6.0 Hz).

^{51}V NMR (158 MHz, CD_3CN): δ (ppm) = -496.87 (s, 6V); -537.50 (s, 6V).

Table S2 Cryo-MS data for **DLD** in acetonitrile

$TBA_xH_y[V_6O_{13}\{(OCH_2)_3CCH_2OCH_2C(CH_2O)_3(P_2V_3W_{15}O_{59})\}_2]$			
Counter-cations	**Charge**	**Calcd. m/z**	**Observed m/z**
TBA_6H_2	6-	1716.50	1716.59
TBA_7H_2	5-	2108.46	2108.44
TBA_8H_1	5-	2156.71	2156.69
TBA_9H_0	5-	2204.97	2204.95
TBA_8H_2	4-	2696.14	2696.12
TBA_9H_1	4-	2756.46	2756.44

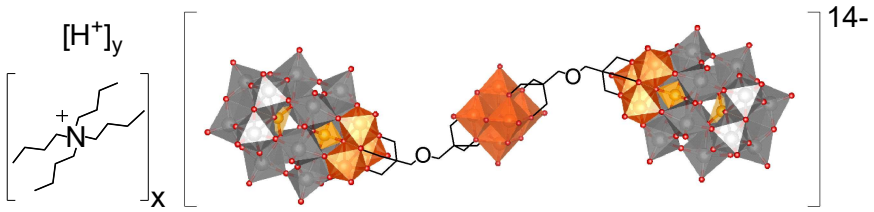

$TBA_xH_y[V_6O_{13}\{(OCH_2)_3CCH_2OCH_2C(CH_2O)_3(P_2W_{15}V_3O_{59})\}_2]$

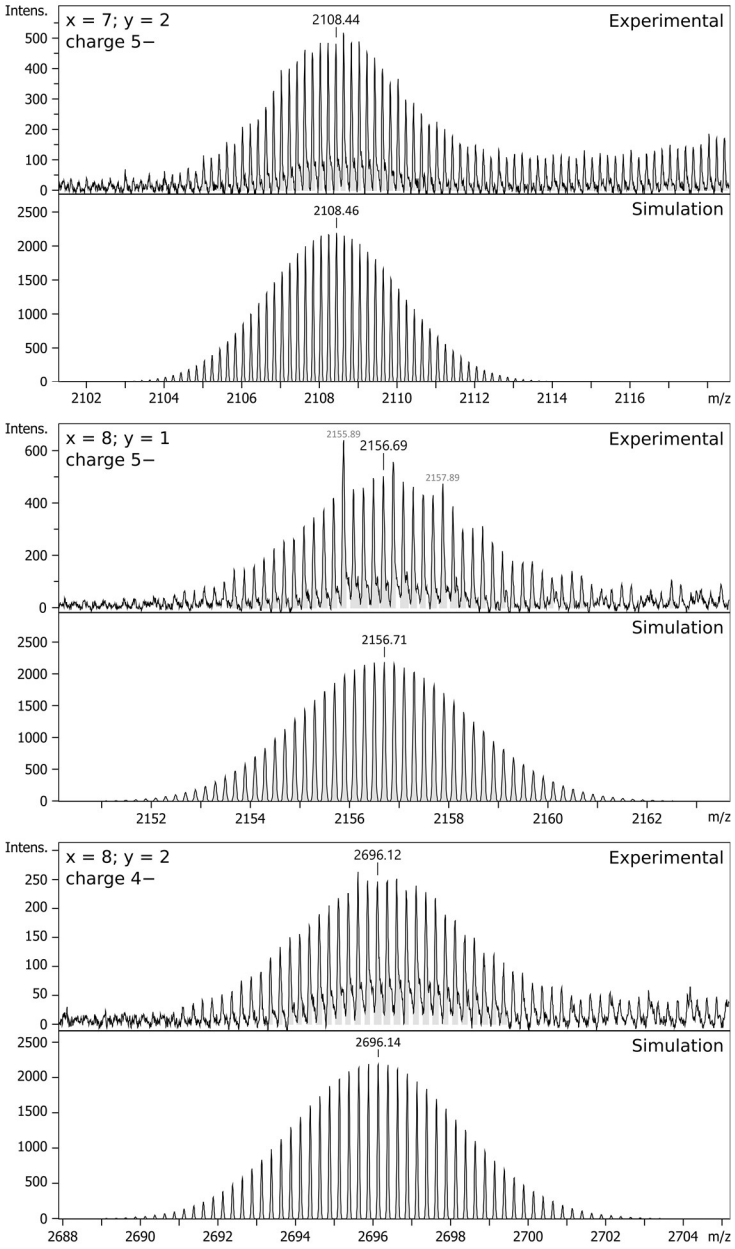

Figure S14 Experimental and simulated cryo-MS spectra for **DLD**.

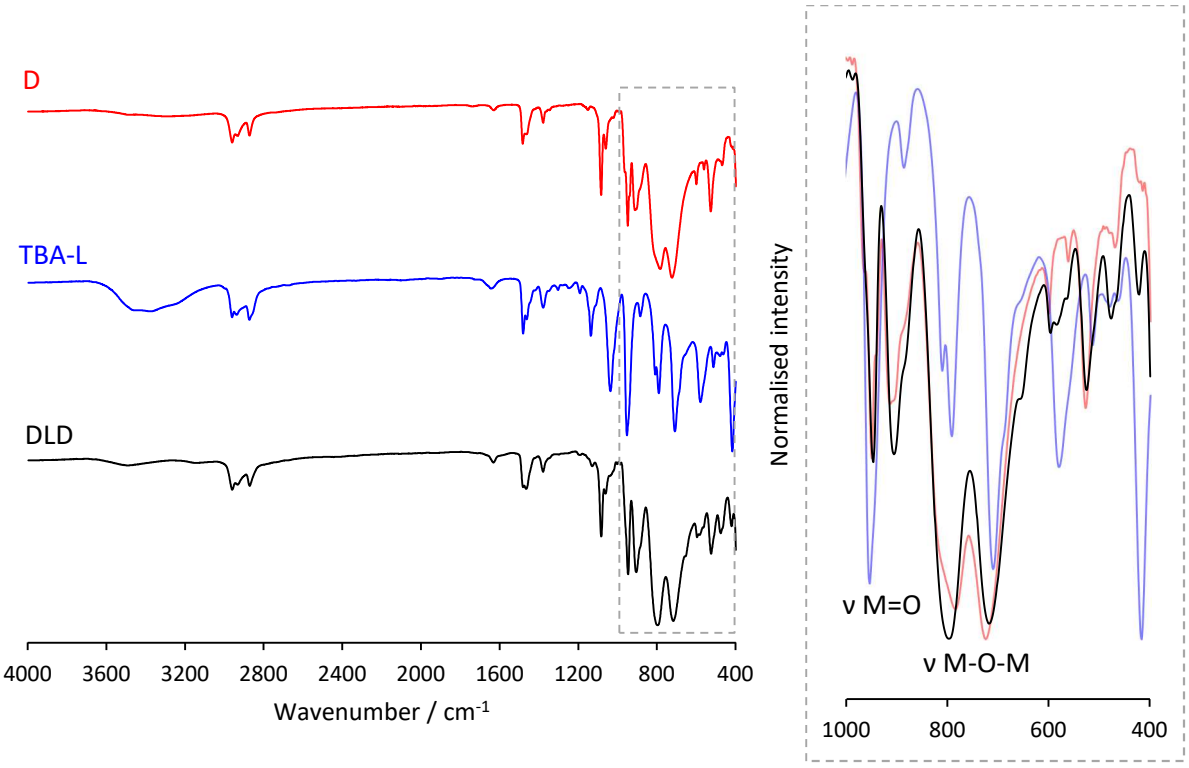

Figure S15 FT-IR spectra of **D** (top; red), **TBA-L** (middle; blue) and **DLD** (bottom; black) with the insert (right) showing the overlayed spectra for the fingerprint region in the range 400 to 1000 cm^{-1} with peaks corresponding to the M=O and M-O-M vibrations of the POM cores (M = V, or W).

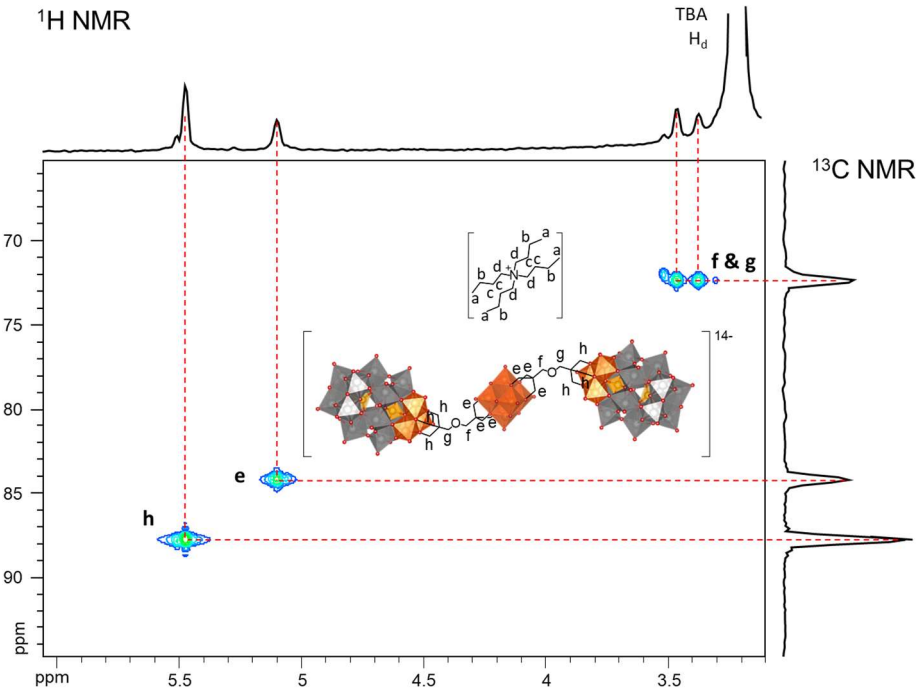

Figure S16 ^{1}H-^{13}C HSQC 2D NMR spectrum of **DLD** in CD_3CN.

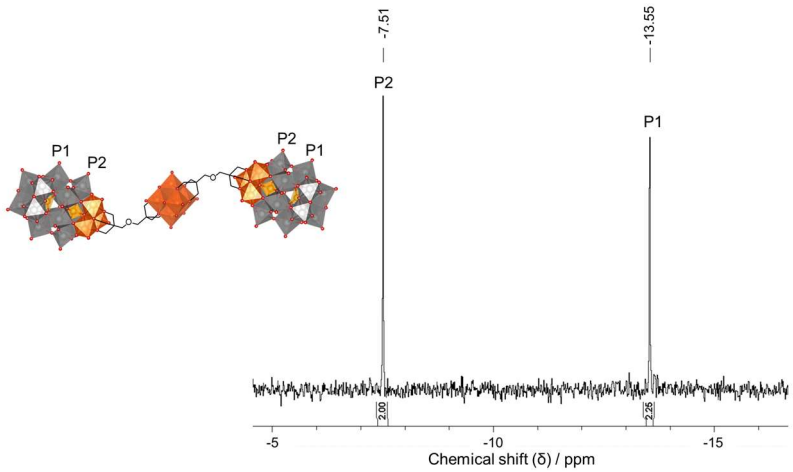

Figure S17 ^{31}P NMR spectrum of **DLD** in CD_3CN.

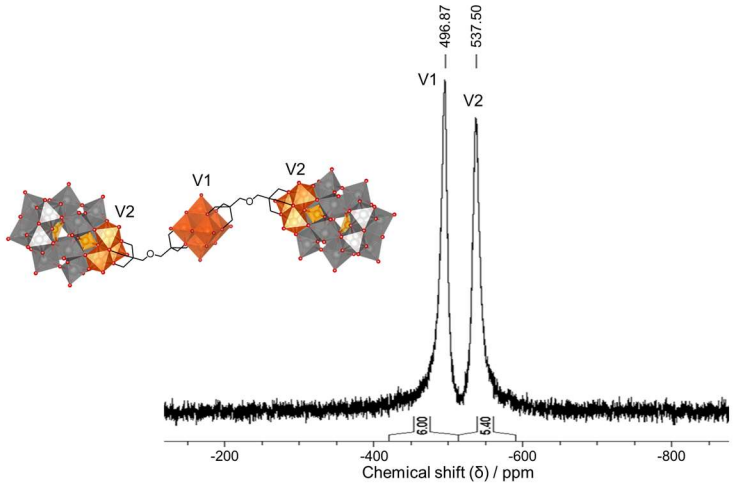

Figure S18 ^{51}V NMR spectrum of **DLD** in CD_3CN.

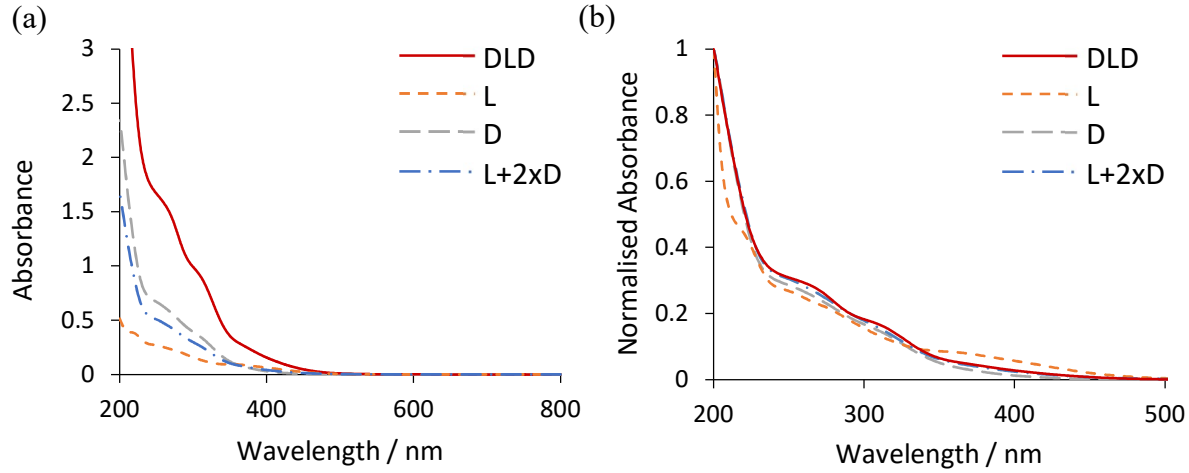

Figure S19 UV-Vis spectra of 10 μM solutions of **DLD**, **L**, **D** and a 1:2 mixture of **L** and **D**: (a) raw and (b) normalised data.

Synthesis of $TBA_{12.4}H_{2.6}[CrMo_6O_{18}\{(OCH_2)_3CCH_2OCH_2C(CH_2O)_3(P_2V_3W_{15}O_{59})\}_2]$ – DCD

DCD was synthesised through a similar procedure to the one used for **DLD** with **TBA-C** (0.1 mmol) instead of **TBA-L**. Yield: 1.04 g, 85.5%

Elemental Analysis (%) for $C_{218.4}H_{481}N_{12.4}O_{150}P_4V_6CrMo_6W_{30}$ (12253.92 $gmol^{-1}$): calcd. = C 21.41, H 3.96, N 1.42, V 2.49, Cr 0.42, Mo 4.70 and W 45.01; found = C 21.54, H 3.96, N 1.37, V 2.46, Cr 0.42, Mo 4.93 and W 45.48.

FT-IR: $\tilde{\nu}$ (cm^{-1}) = 3486 (ν O-H, w), 3134 (w), 2960 (ν C-H, m), 2933 (ν C-H, m), 2871 (ν C-H, m), 1632 (w), 1481 (δ C-H, m), 1465 (δ C-H, m), 1379 (δ C-H, w), 1191 (w), 1128 (ν C-O, m), 1083 (ν P-O, m), 1062 (m), 1020 (ν C-O, w), 989 (w), 947 (ν M=O, s), 902 (ν M=O, s), 795 (ν M-O-M, vs), 719 (ν V-O-V, vs), 658 (ν Mo-O-Mo, vs), 598 (s), 564 (s), 524 (s), 479 (s), 465 (s), 421 (s). M = Mo, V or W.

^{31}P NMR (162 MHz, CD_3CN): δ (ppm) = -7.58 (s, 2P, $\Delta\nu_{½}$ = 11.1 Hz); -13.51 (s, 2P, $\Delta\nu_{½}$ = 3.9 Hz).

^{51}V NMR (105 MHz, CD_3CN): δ (ppm) = -538.59 (s).

Table S3 Cryo-MS data for **DCD** in acetonitrile

$TBA_xH_y[CrMo_6O_{18}\{(OCH_2)_3CCH_2OCH_2C(CH_2O)_3(P_2V_3W_{15}O_{59})\}_2]$

Counter-cations	Charge	Calcd. m/z	Observed m/z
TBA_7H_2	6-	1824.00	1823.99
TBA_8H_2	5-	2237.25	2237.24
TBA_9H_1	5-	2285.71	2285.69
TBA_9H_2	4-	2857.39	2857.37

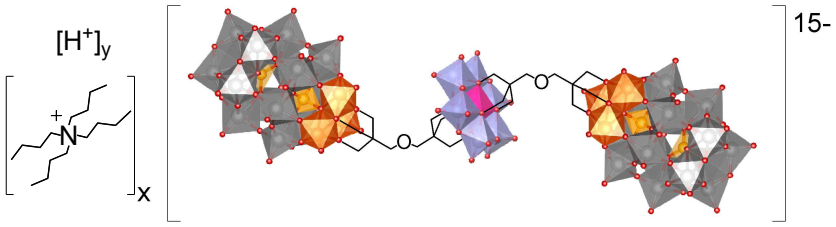

$TBA_xH_y[CrMo_6O_{18}\{(OCH_2)_3CCH_2OCH_2C(CH_2O)_3(P_2W_{15}V_3O_{59})\}_2]$

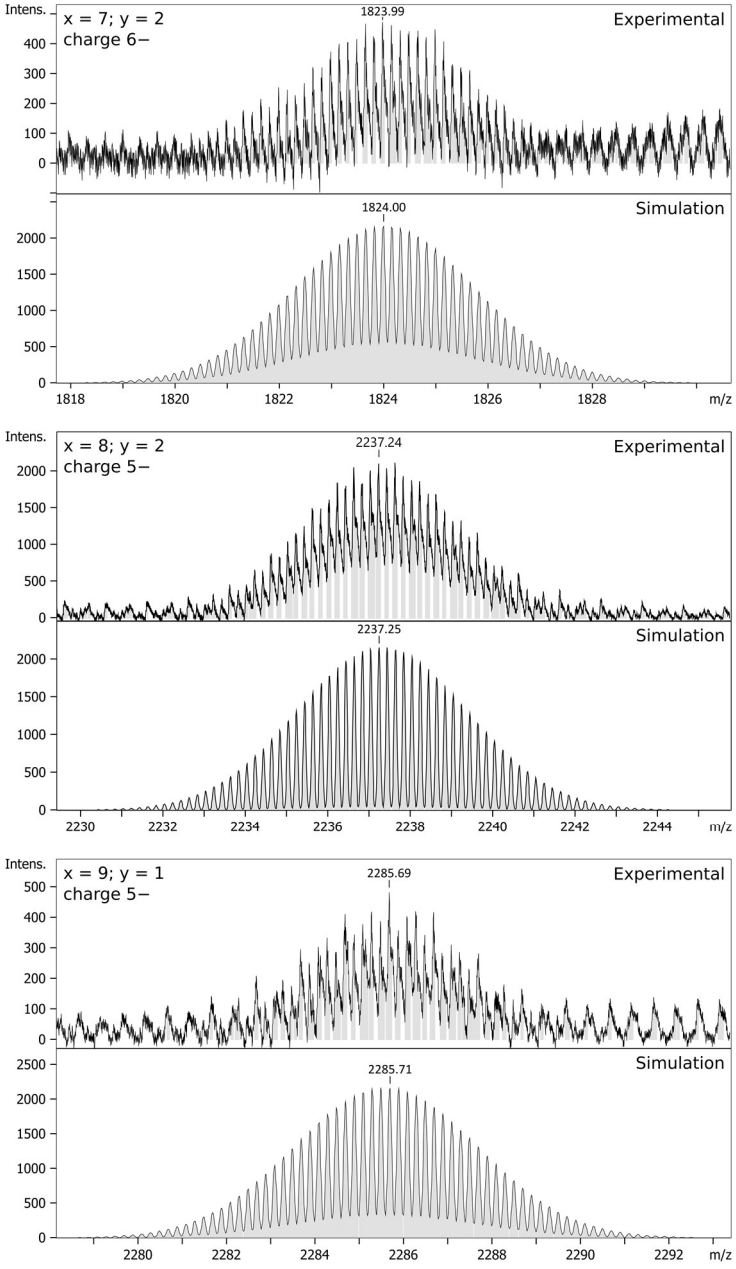

Figure S20 Experimental and simulated cryo-MS spectra for **DCD**.

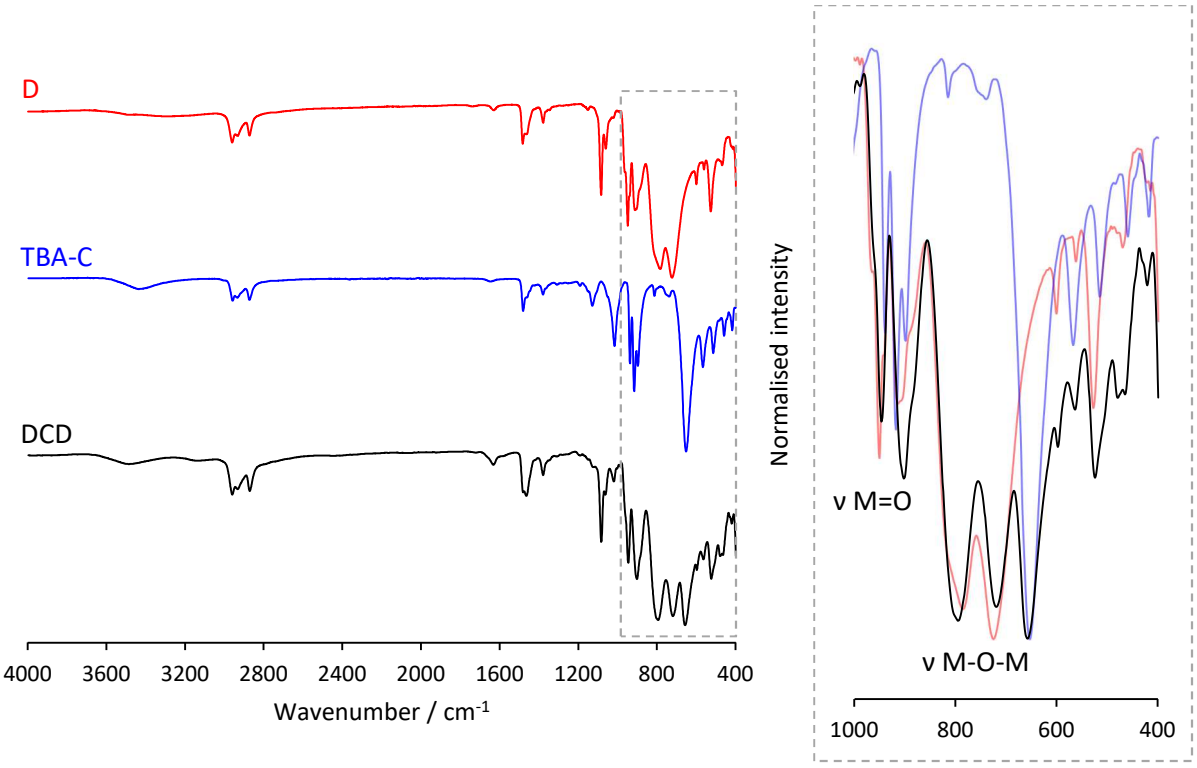

Figure S21 FT-IR spectra of **D** (top; red), **TBA-C** (middle; blue) and **DCD** (bottom; black) with the insert (right) showing the overlayed spectra for the fingerprint region in the range 400 to 1000 cm^{-1} with peaks corresponding to the M=O and M-O-M vibrations of the POM cores (M = Mo, V, or W).

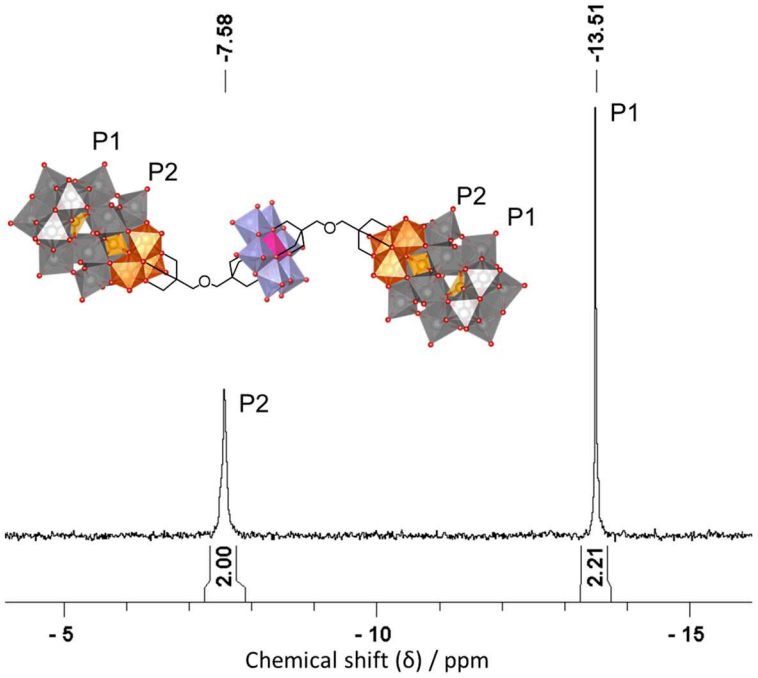

Figure S22 ^{31}P NMR spectrum of **DCD** in CD_3CN.

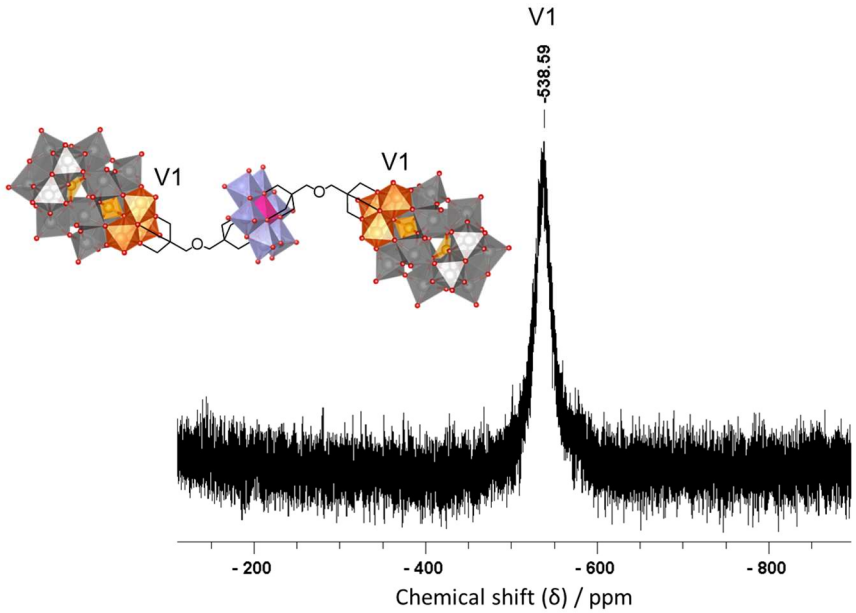

Figure S23 ^{51}V NMR spectrum of **DCD** in CD_3CN.

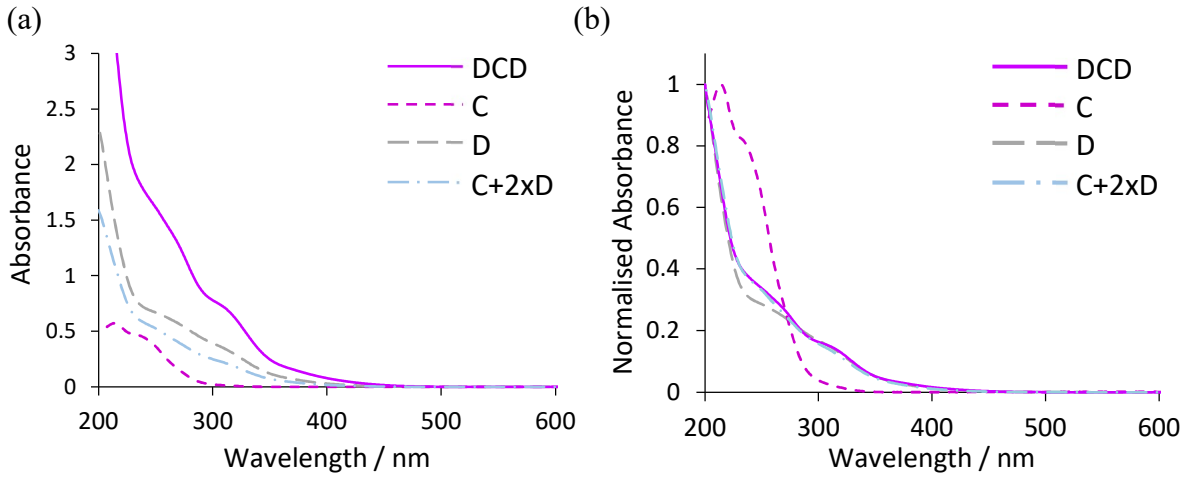

Figure S24 UV-Vis spectra of 10 μM solutions of **DCD**, **C**, **D** and a 1:2 mixture of **C** and **D**: (a) raw and (b) normalised data.

Synthesis of $TBA_8[V_6O_{13}\{(OCH_2)_3CCH_2OCH_2C(CH_2O)_3(Al(OH)_3Mo_6O_{18})\}_2]$ – ALA
Dissolved $Na_3(H_2O)_6[Al(OH)_6Mo_6O_{18}]\cdot 2H_2O$ (0.207 mmol) in 1.65 mL of demineralised water by ultrasonication in a 4 mL glass vial and then added **Na-L** (0.103 mmol). After sealing the vial with a septum, it was placed in a heating block at 100 °C for 3 h. The reaction mixture was then allowed to cool down and tetrabutylammonium bromide (1.03 mmol) was added resulting in instant precipitation of the desired product. The precipitate was washed with demineralised water and it was then dissolved in a minimum amount of acetonitrile to form a solution which was then added dropwise to 10 mL of diethyl ether. The oily red solution that formed was washed twice with 8 mL of ethanol and 8 mL of diethyl ether until a dispersed yellow powder was observed. It was then separated by centrifugation and dried under dynamic vacuum overnight at 50 °C. Yield: 0.35 g, 70.3%

Elemental Analysis (%) for $C_{148}H_{326}N_8O_{69}Al_2Mo_6V_6$ (4833.08 $gmol^{-1}$): calcd. = C 36.78, H 6.80, N 2.32, Al 1.12, Mo 23.82, V 6.32; found = C 35.96, H 6.72, N 1.90, Al 1.05, Mo 23.42, V 6.43.

FT-IR: $\tilde{\nu}$ (cm^{-1}) = 3434 (ν O-H, w), 2960 (ν C-H, m), 2934 (ν C-H, m), 2873 (ν C-H, m), 1643 (w), 1480 (δ C-H, m), 1380 (δ C-H, w), 1195 (w), 1132 (ν C-O, m), 1110 (w), 1035 (ν C-O, m), 939 (ν M=O, s), 917 (ν Mo=O, s), 899 (ν Mo=O, m), 806 (ν V-O-V, s), 717 (ν V-O-V, s), 649 (ν Mo-O-Mo, vs), 575 (s), 511 (s), 490 (s), 451 (s), 417 (s). M = Mo or V.

^{1}H NMR (600 MHz, CD_3CN): δ (ppm) = 0.99 (t, 96 H, TBA CH_3), 1.40 (m, 64 H, TBA CH_2), 1.66 (m, 64 H, TBA CH_2), 3.03 (s, 4 H, CH_2-O-CH_2), 3.18 (m, 64 H, N-TBA CH_2), 3.23 (s, 4 H, CH_2-O-CH_2); 4.50 (s, 12 H, CH_2-O-Al), 4.95 (s, 12 H, CH_2-O-V_6).

^{13}C NMR (151 MHz, CD_3CN): δ (ppm) = 13.93 (TBA CH_3), 20.37 (TBA CH_2), 24.45 (TBA CH_2), 41.10 (C(CH_2O-)$_3$), 59.34 (TBA N-CH_2), 75.10 (CH_2-O-CH_2), 76.89 (CH_2-O-Al), 84.59 (CH_2-O-V_6).

^{51}V NMR (158 MHz, CD_3CN): δ (ppm) = -496.52 (s).

^{27}Al NMR (104 MHz, CD_3CN): δ (ppm) = 15.69 (s).

Table S4 Negative mode ESI-MS data for **ALA** in acetonitrile

$TBA_xH_y[V_6O_{13}\{(OCH_2)_3CCH_2OCH_2C(CH_2O)_3(Al(OH)_3Mo_6O_{18})\}_2]\cdot(CH_3CN)_a(H_2O)_b$

Counter-cations	Solvent	Charge	Calcd. m/z	Observed m/z
TBA_5H_0	$(ACN)_3(H_2O)_1$	3-	1415.61	1415.15
TBA_1H_5	$(ACN)_2(H_2O)_0$	2-	1611.43	1610.39
TBA_2H_4	$(ACN)_0(H_2O)_{-1}$	2-	1682.15	1681.52
TBA_2H_4	$(ACN)_3(H_2O)_0$	2-	1752.74	1753.12
TBA_3H_3	$(ACN)_1(H_2O)_{-1}$	2-	1823.41	1824.25
TBA_3H_3	$(ACN)_4(H_2O)_0$	2-	1894.23	1894.11

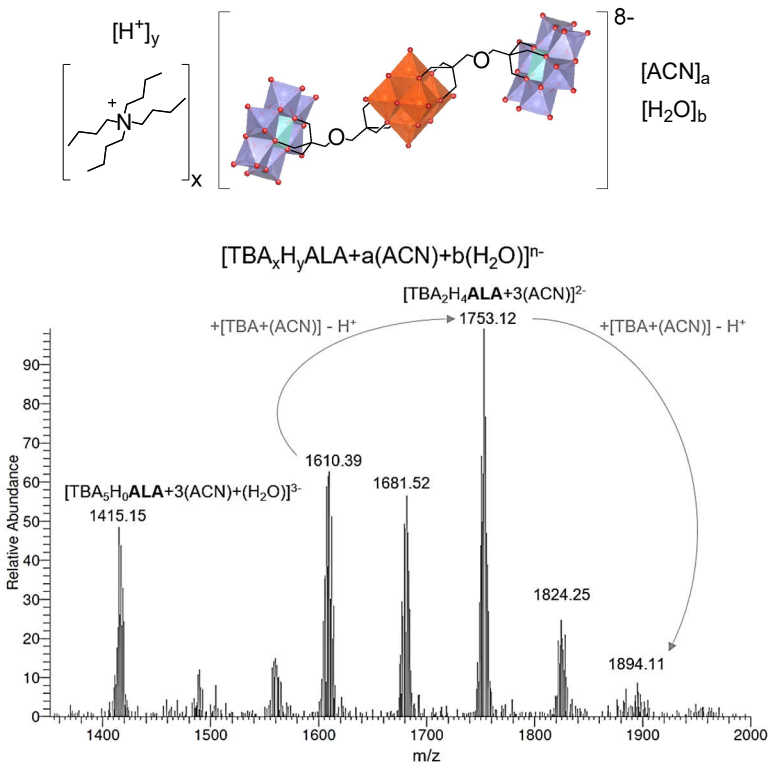

Figure S25 Negative mode ESI-MS spectrum of **ALA**.

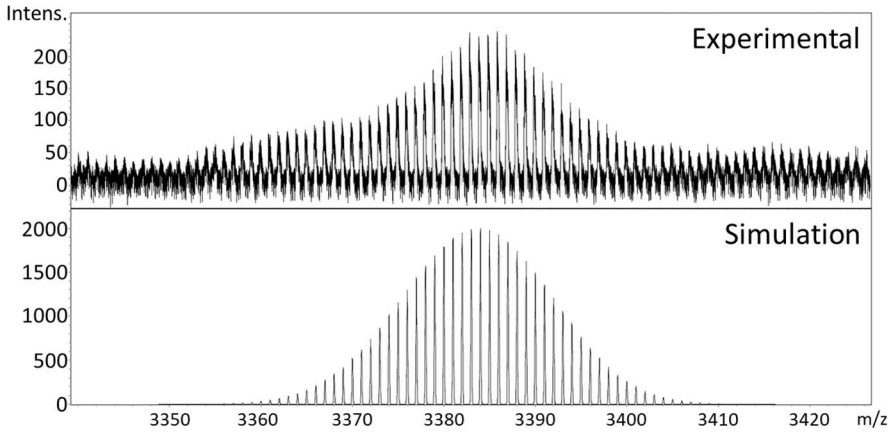

Figure S26 Experimental cryo-MS spectrum of **ALA** showing a profile centred at *m/z* 3383.87, which is close to the simulated spectrum centred at *m/z* 3384.05 corresponding to $\{TBA_2H_5[V_6O_{13}\{(OCH_2)_3CCH_2OCH_2C(CH_2O)_3(AlMo_6O_{18}(OH)_3)\}_2]\}^{1-}$.

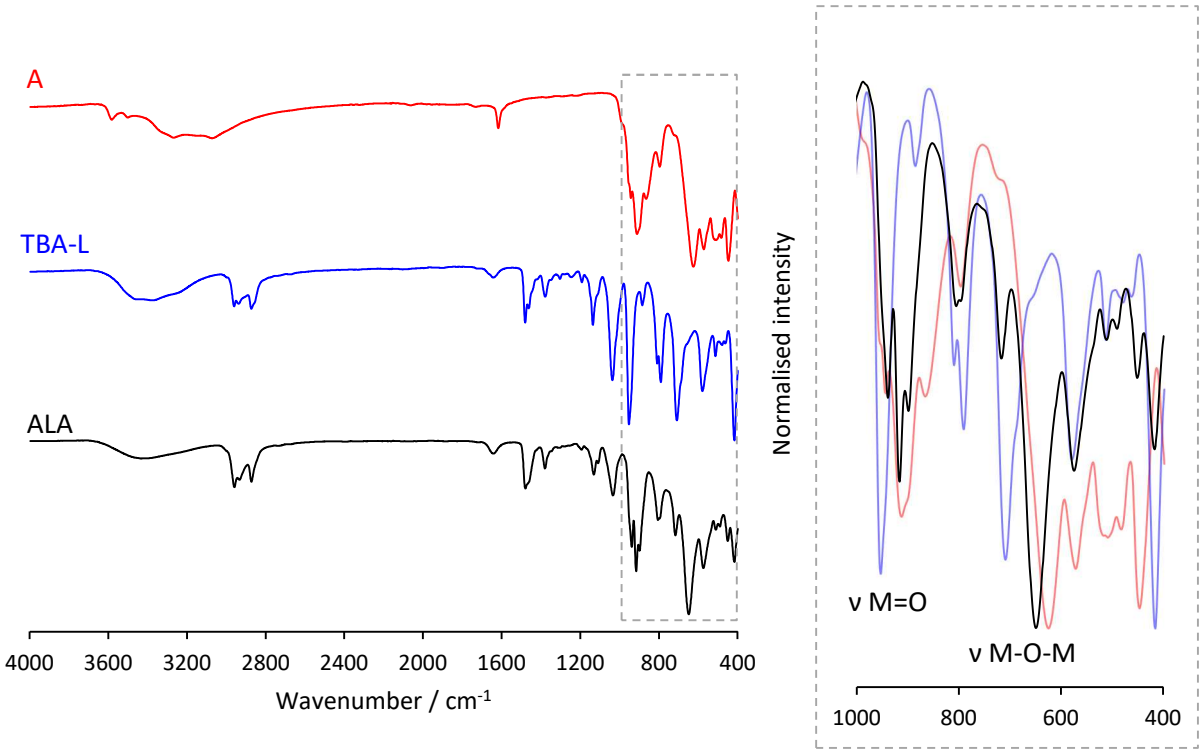

Figure S27 FT-IR spectra of **A** (top; red), **TBA-L** (middle; blue) and **ALA** (bottom; black).

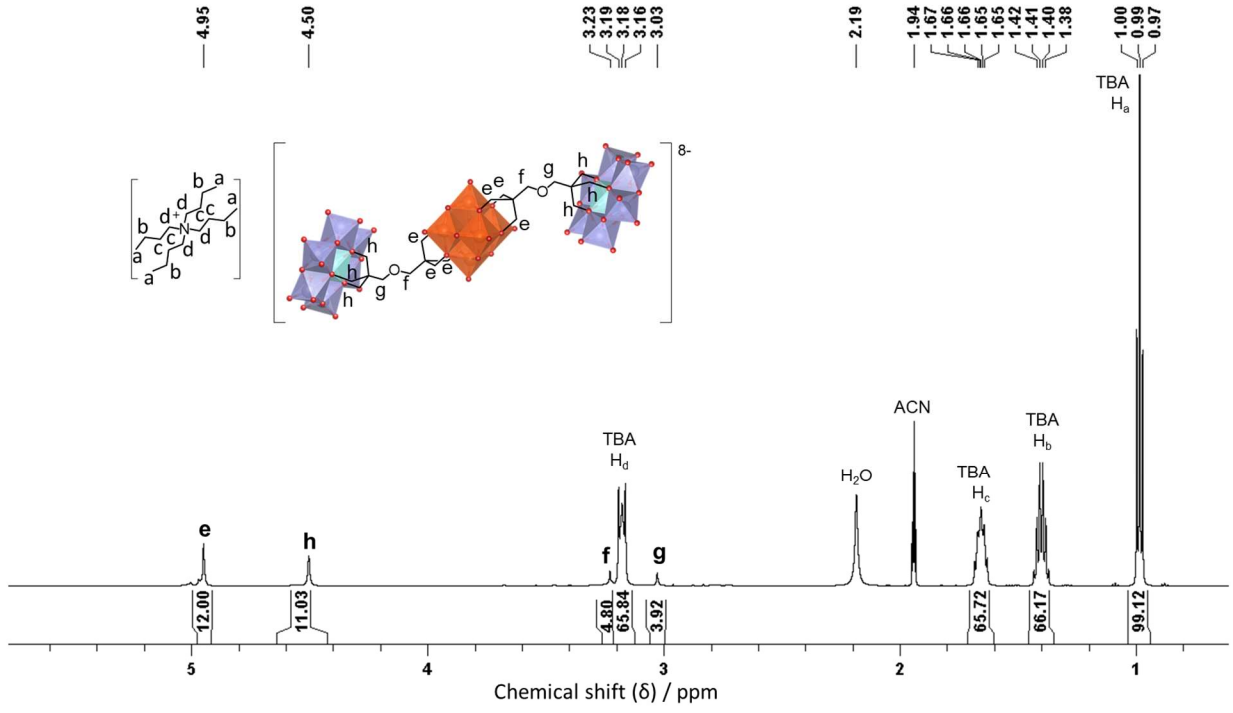

Figure S28 ^{1}H NMR spectrum of **ALA** in CD_3CN.

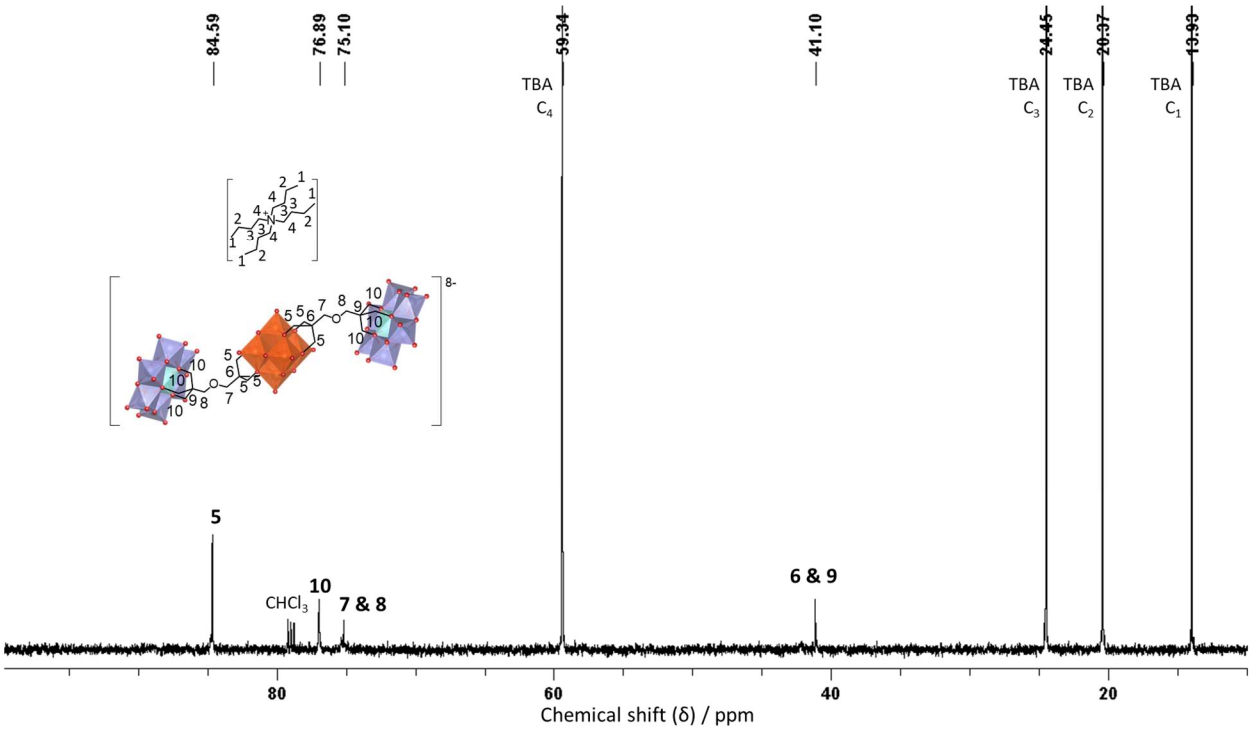

Figure S29 ^{13}C NMR spectrum of **ALA** in CD_3CN.

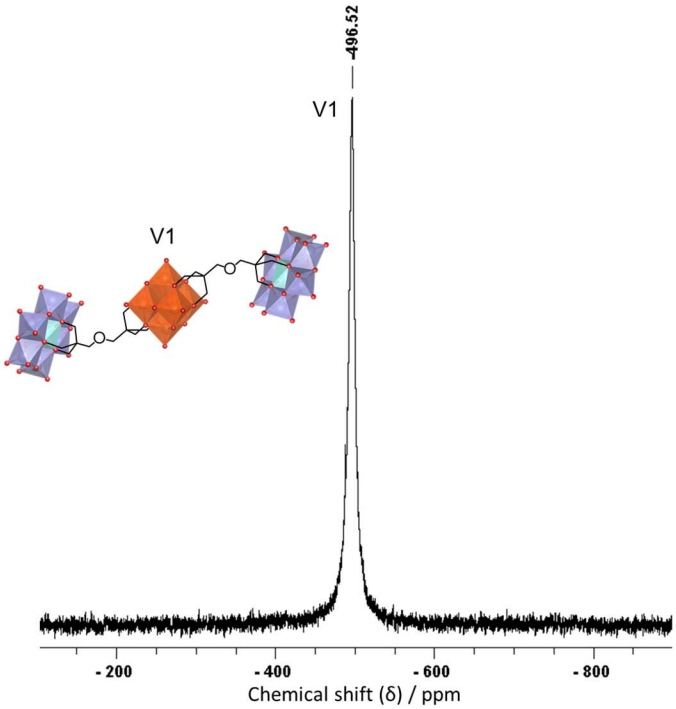

Figure S30 ^{51}V NMR spectrum of **ALA** in CD_3CN.

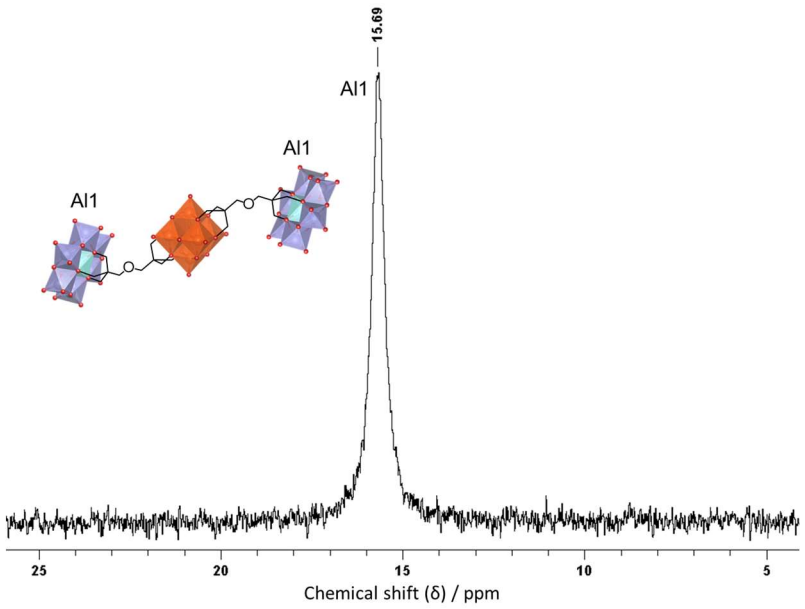

Figure S31 ^{27}Al NMR spectrum of **ALA** in CD_3CN.

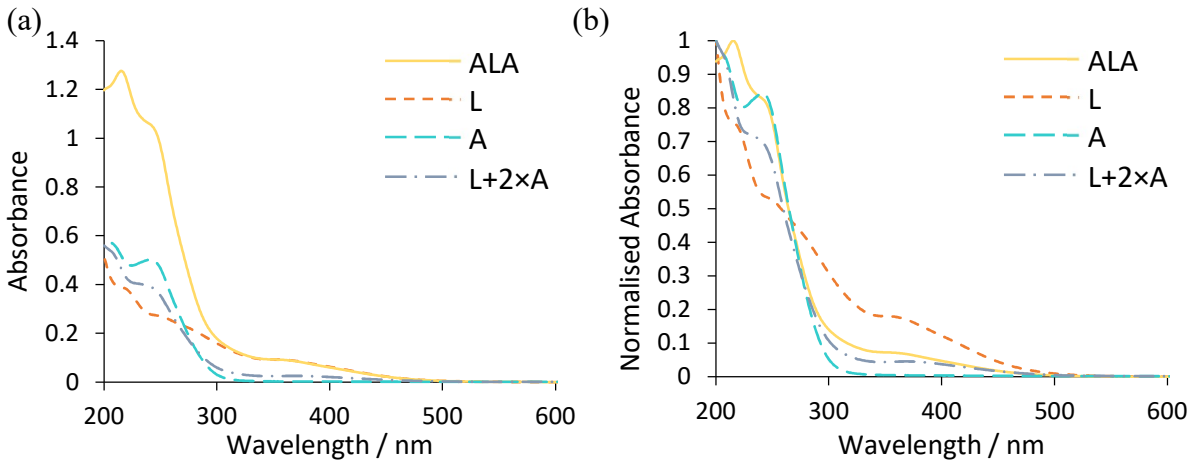

Figure S32 UV-Vis spectra of 10 μM solutions of **ALA**, **L**, **A** and a 1:2 mixture of **L** and **A**: (a) raw and (b) normalised data.

Synthesis of $TBA_9[CrMo_6O_{18}\{(OCH_2)_3CCH_2OCH_2C(CH_2O)_3(Al(OH)_3Mo_6O_{18})\}_2]$ – ACA

ACA was synthesised using a similar procedure to that used for **ALA** with **Na-C** (0.027 mmol) instead of **Na-L**. Yield: 0.127 g, 85.9%

Elemental Analysis (%) for $C_{164}H_{362}N_9O_{74}Al_2Mo_{18}Cr$ (5477.52 $gmol^{-1}$): calcd. = C 35.96, H 6.66, N 2.30, Mo 31.53, Cr 0.95; found = C 35.62, H 6.62, N 1.84, Mo 35.57, Cr 0.91

FT-IR: $\tilde{\nu}$ (cm^{-1}) = 3437 (ν O-H, w), 2959 (ν C-H, m), 2934 (ν C-H, m), 2873 (ν C-H, m), 1646 (w), 1471 (δ C-H, m), 1381 (δ C-H, w), 1198 (w), 1131 (ν C-O, m), 1111 (m), 1018 (ν C-O, m), 967 (w), 937 (ν Mo=O, s), 916 (ν Mo=O, s), 899 (ν Mo=O, s), 823 (w), 808 (w), 736 (m), 650 (ν Mo-O-Mo, vs), 566 (s), 508 (s), 451 (s), 417 (m).

^{13}C NMR (151 MHz, CD_3CN): δ (ppm) = 14.02 (TBA CH_3), 20.44 (TBA CH_2), 24.42 (TBA CH_2), 42.05 ($C(CH_2O\text{-})_3$), 59.29 (TBA N-CH_2), 77.31 (CH_2-O-Al).

^{27}Al NMR (104 MHz, CD_3CN): δ (ppm) = 15.64 (s).

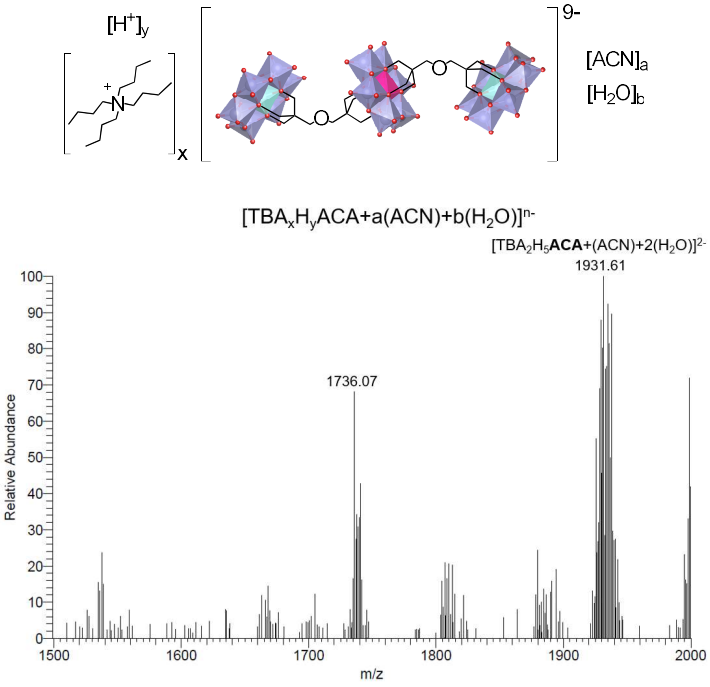

Figure S33 Negative mode ESI-MS spectrum of **ACA** showing a profile centred at *m/z* 1931.61, which matches $\{TBA_2H_5[CrMo_6O_{18}\{(OCH_2)_3CCH_2OCH_2C(CH_2O)_3(AlMo_6O_{18}(OH)_3)\}_2](CH_3CN)(H_2O)_2\}^{2-}$ with a calculated average isotopic *m/z* of 1931.40.

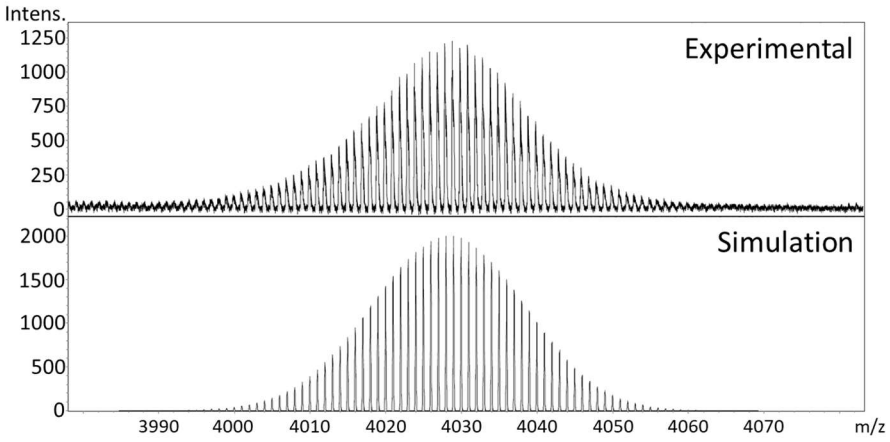

Figure S34 Experimental cryo-MS spectrum of **ACA** showing a profile centred at *m/z* 4027.85, which is close to the simulated spectrum centred at *m/z* 4028.03 corresponding to $\{TBA_3H_5[CrMo_6O_{18}\{(OCH_2)_3CCH_2OCH_2C(CH_2O)_3(AlMo_6O_{18}(OH)_3)\}_2]\}^{1-}$.

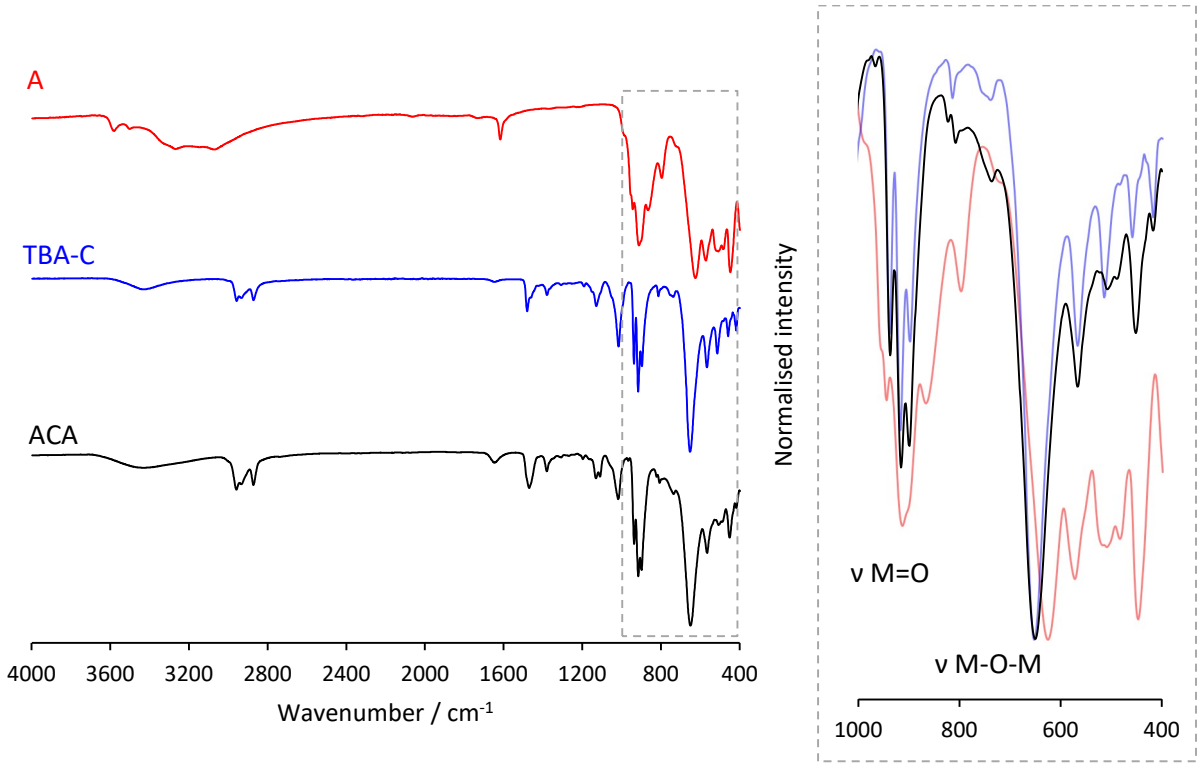

Figure S35 FT-IR spectra of **A** (top; red), **TBA-C** (middle; blue) and **ACA** (bottom; black) powder.

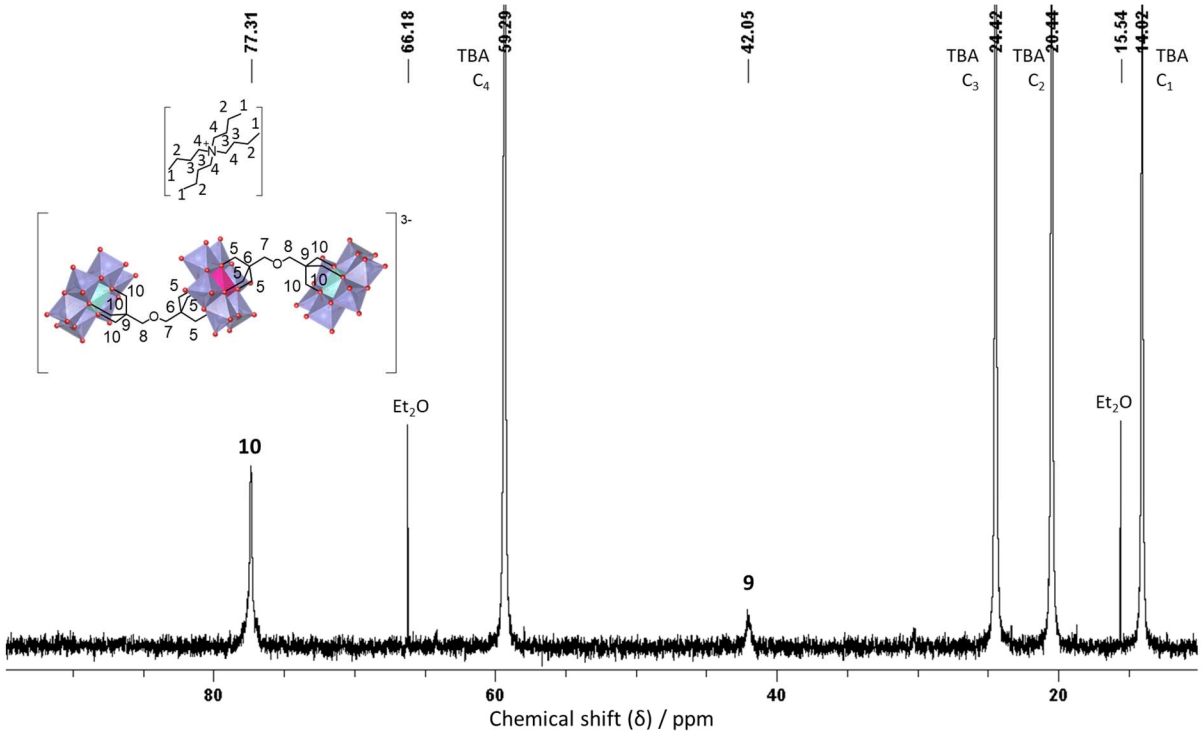

Figure S36 ^{13}C NMR spectrum of **ACA** in CD_3CN.

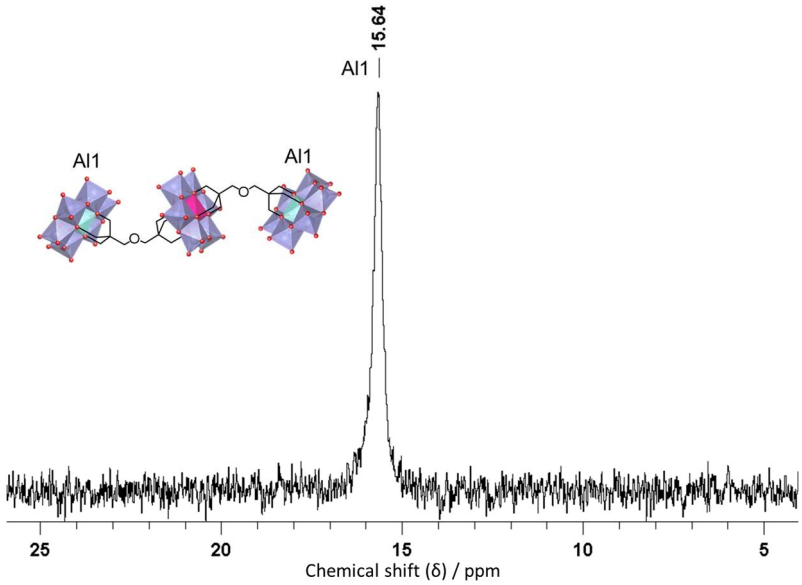

Figure S37 ^{27}Al NMR spectrum of **ACA** in CD_3CN.

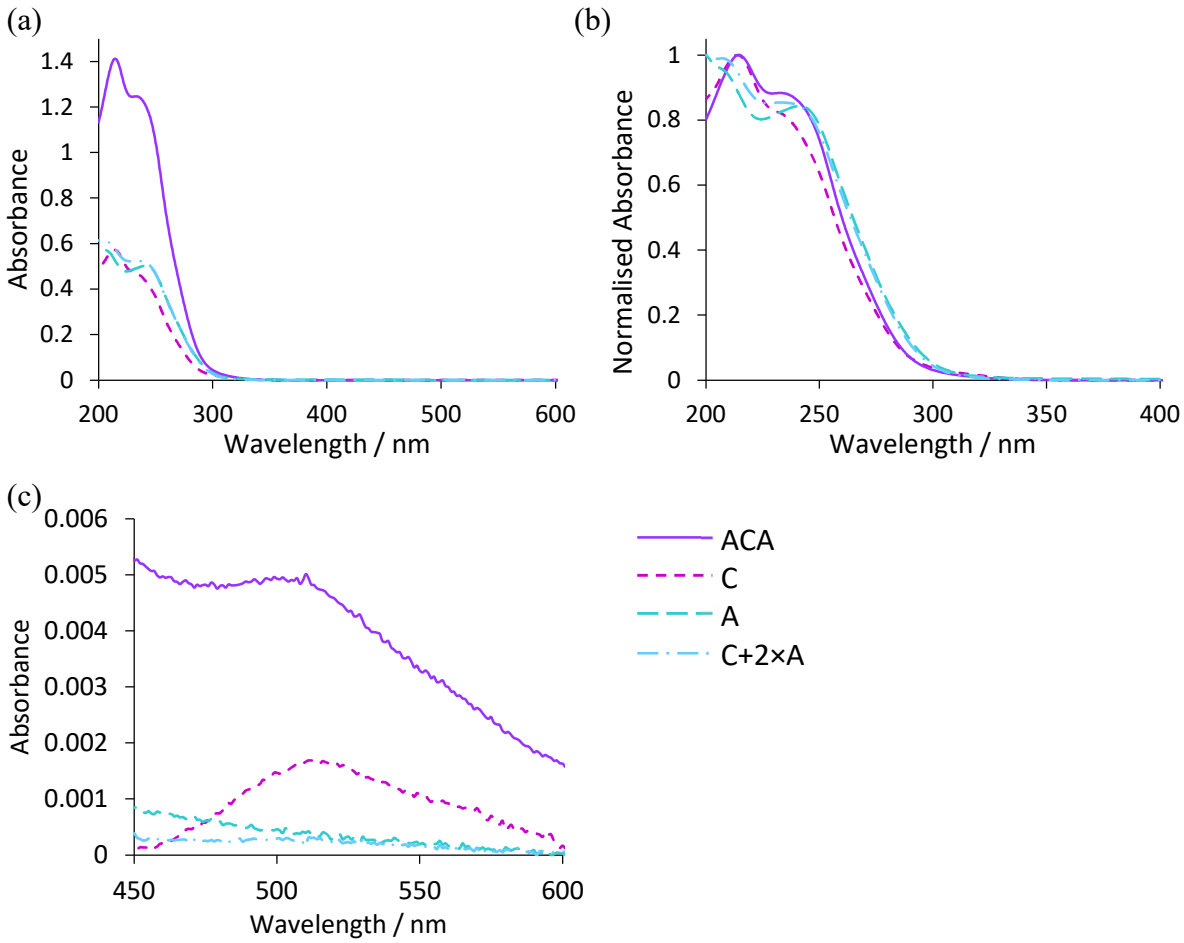

Figure S38 UV-Vis spectra of 10 μM solutions of **ACA**, **C**, **A** and a 1:2 mixture of **C** and **A**: (a) raw and (b) normalised data. (c) Raw data showing the weak d-d transition peak.

References

1 CrysAlis PRO (2012). Agilent Technologies UK Ltd, Yarnton, Oxfordshire, England.

2 O. V. Dolomanov, L. J. Bourhis, R. J. Gildea, J. A. K. Howard and H. Puschmann, OLEX2 : a complete structure solution, refinement and analysis program, *J. Appl. Crystallogr.*, 2009, **42**, 339–341.

3 G. M. Sheldrick, SHELXT – Integrated space-group and crystal-structure determination, *Acta Crystallogr. Sect. A Found. Adv.*, 2015, **71**, 3–8.

4 G. M. Sheldrick, Crystal structure refinement with SHELXL, *Acta Crystallogr. Sect. C Struct. Chem.*, 2015, **71**, 3–8.

5 P. Wu, P. Yin, J. Zhang, J. Hao, Z. Xiao and Y. Wei, Single-side organically functionalized anderson-type polyoxometalates, *Chem. - A Eur. J.*, 2011, **17**, 12002–12005.

6 R. G. Finke, B. Rapko, R. J. Saxton and P. J. Domaille, Trisubstituted heteropolytungstates as soluble metal oxide analogs. III. Synthesis, characterization, phosphorus-31, silicon-29, vanadium-51, and 1- and 2-D tungsten-183 NMR, deprotonation, and proton mobility studies of organic solvent solute forms of Hx, *J. Am. Chem. Soc.*, 1986, **108**, 2947–2960.

7 V. Shivaiah and S. K. Das, Supramolecular assembly based on a heteropolyanion: Synthesis and crystal structure of Na3(H2O)6[Al(OH)6Mo6O18]·2H2O, *J. Chem. Sci.*, 2005, **117**, 227–233.

8 P. Wu, J. Chen, P. Yin, Z. Xiao, J. Zhang, A. Bayaguud and Y. Wei, Solvent-induced supramolecular chirality switching of bis-(trisalkoxy)-hexavanadates, *Polyhedron*, 2013, **52**, 1344–1348.

9 D. E. Salazar Marcano, S. Lentink, M. A. Moussawi and T. N. Parac-Vogt, Solution Dynamics of Hybrid Anderson–Evans Polyoxometalates, *Inorg. Chem.*, 2021, **60**, 10215–10226.